Angularity event shapes in High Energy Scatterings

Tanmay Maji

NIT Kurukshetra

08 Feb. 2022

Coauthors: Jiawei Zhu, Daekyoung Kang, Jun Gao

International Workshop on Probing Hadron Structure at the Electron-Ion Collider

ICTS International Centre for Theoretical Sciences

TATA INSTITUTE OF FUNDAMENTAL RESEARCH

Talk organized as…

- Introduction: Jet Event Shapes and angularity
- Event Shapes in DIS
    - Angularity beam functions at NNLL
    - Angularity differential cross-section at NNLL
    - Predictions for future EIC
- Angularity in H -> gg decay at NNLL'
- Conclusion

Jets and Jet Event Shapes?

- In high energy scattering, the most common final states are collimated branches of strongly interacting particles, called jet.

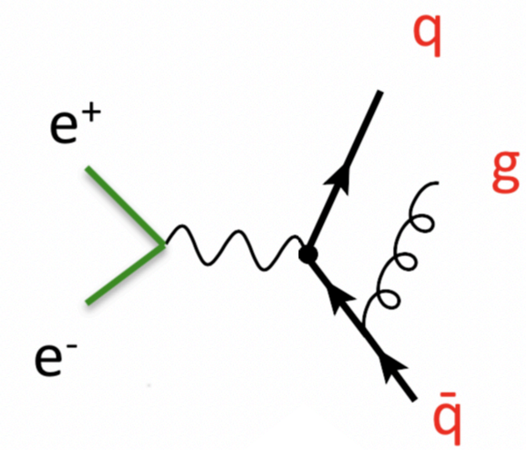

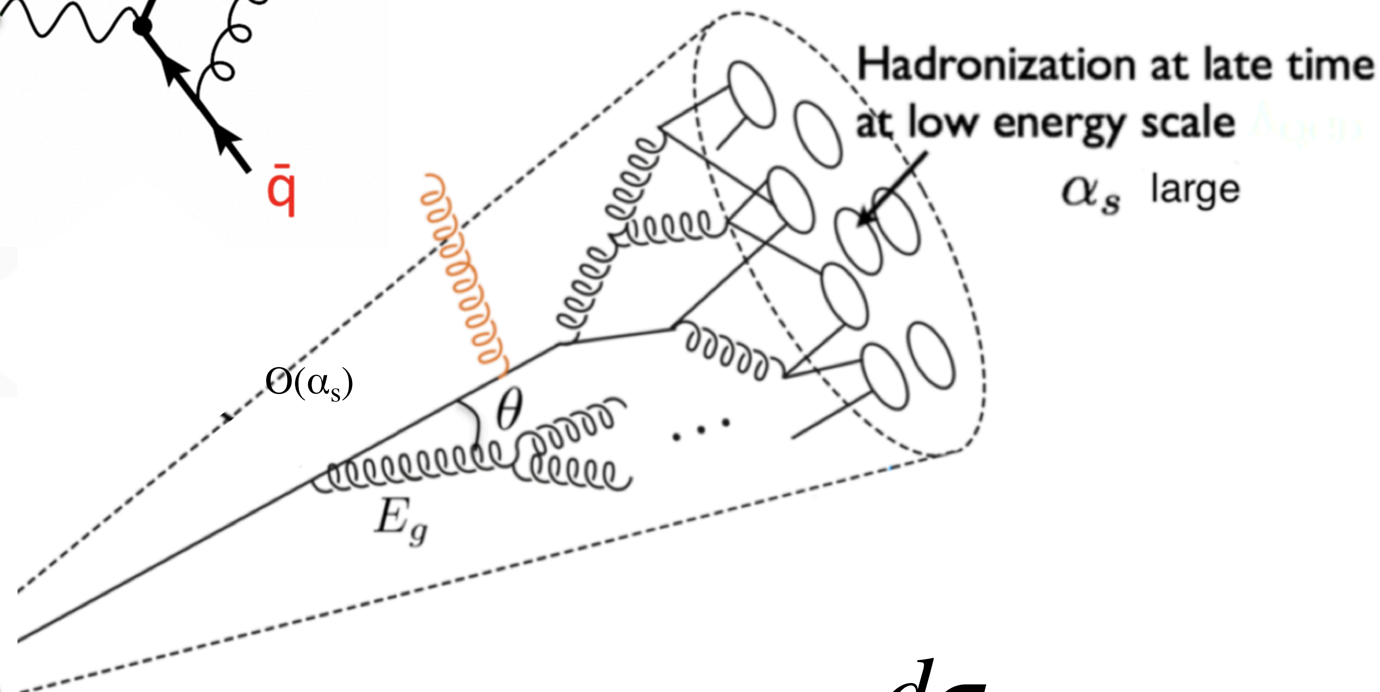

3-jet event: discovery of gluon

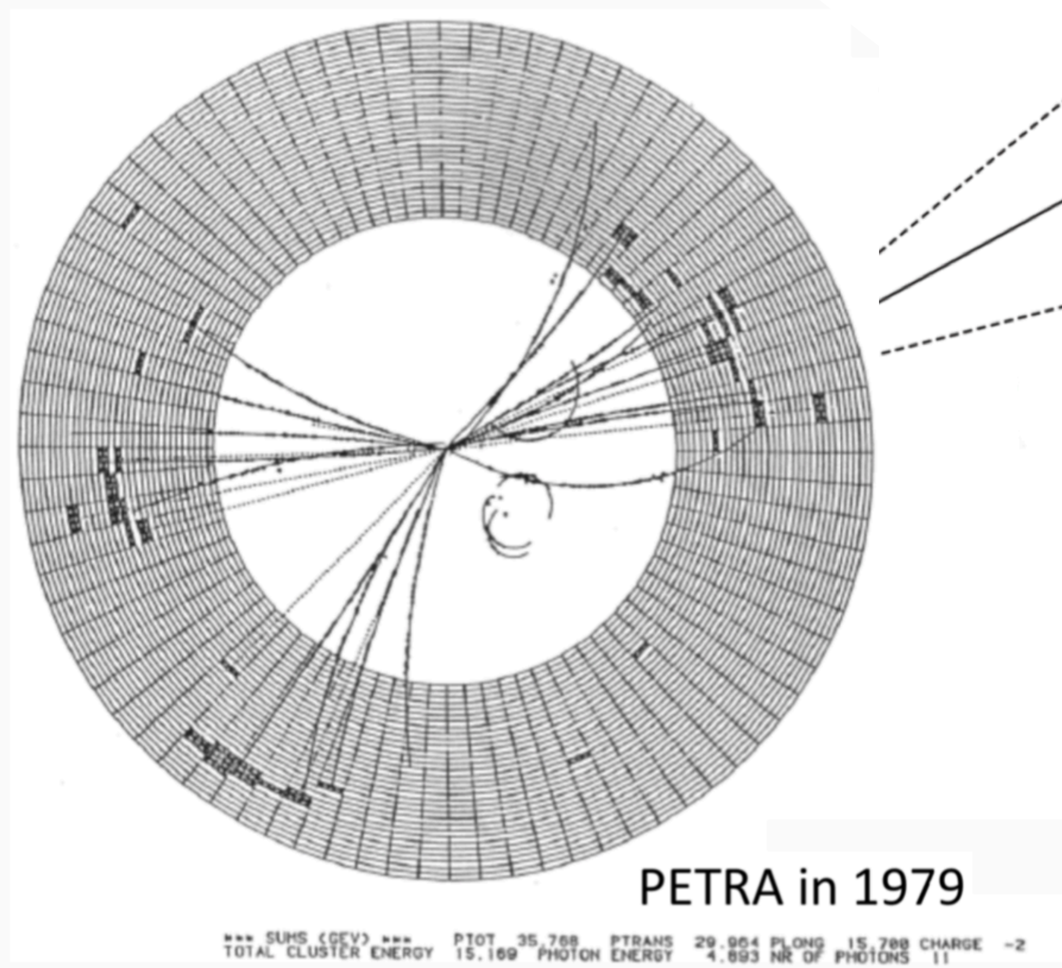

$$\frac{d\sigma}{dx\,dQ^2\,d\tau_a} = ??$$

Jet Observables are called

Event Shapes

e.g., Thrust, Jet Broadening, Angularity…

Thrust: Characterizes the geometry of collision

$$\tau = \frac{2}{Q} \sum_{i\in\mathcal{X}} \left|\mathbf{p}_\perp^i\right| e^{-|\eta_i|}$$

Rapidity: $\eta = \frac{1}{2}\ln\left(\frac{p^-}{p^+}\right)$

Thrust: Characterizes the geometry of collision

$$\tau = \frac{2}{Q} \sum_{i \in \mathcal{X}} \left| \mathbf{p}_{\perp}^{i} \right| e^{-|\eta_i|}$$

Rapidity: $\eta = \frac{1}{2} \ln \left(\frac{p^-}{p^+} \right)$

An example:

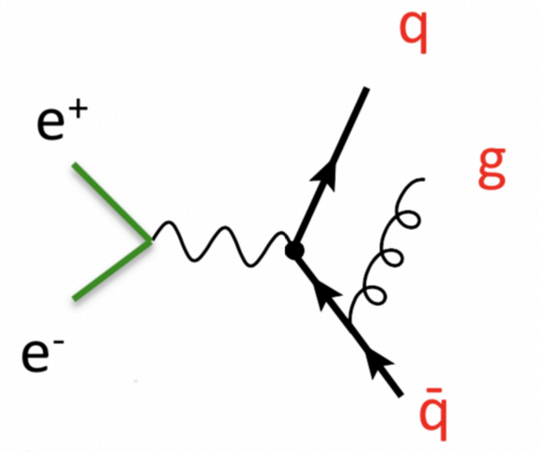

$$\begin{aligned} n &= (1,0,0,1) \\ \bar{n} &= (1,0,0,-1) \end{aligned}$$

$$= \frac{2}{Q^2} \sum_{i \in \chi} min\{p_i.n, p_i.\bar{n}\}$$

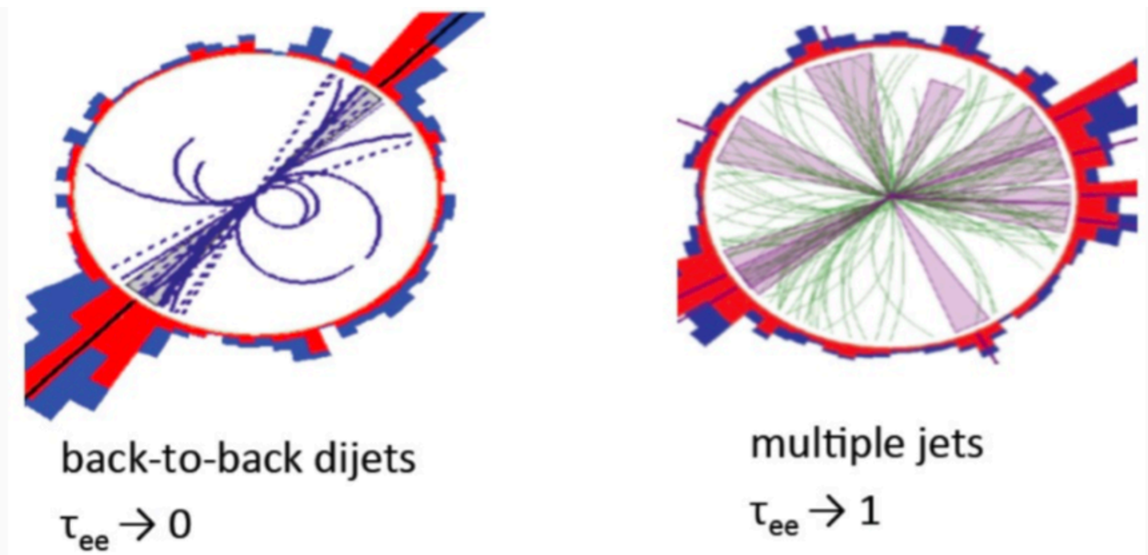

Angularity Event Shapes

[C. F. Berger, T. Kucs and G. F. Sterman' 2003]

$$\tau_a = \frac{2}{Q} \sum_{i \in \mathcal{X}} \left|\mathbf{p}_\perp^i\right| e^{-|\eta_i|(1-a)}$$

Depends on continuous parameter

$$\eta = \frac{1}{2} \ln\left(\frac{p^-}{p^+}\right)$$

A more general event shape!
provide access from thrust to jet broadening in continuous manner

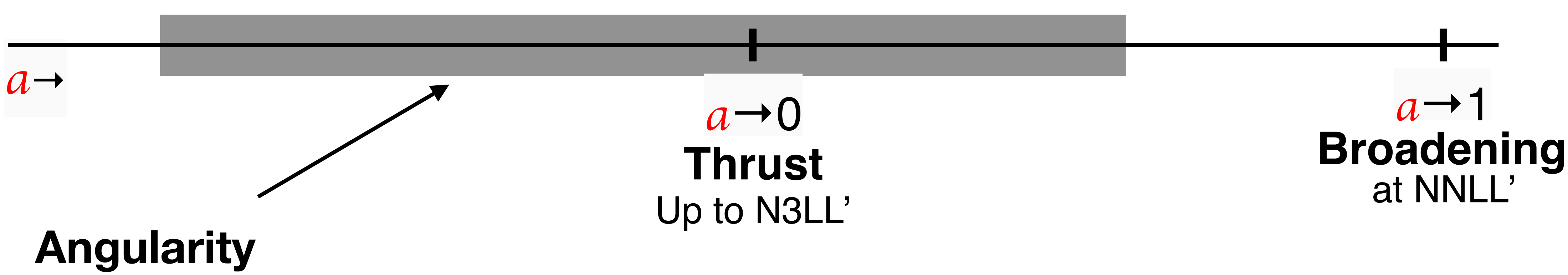

Angularity Event Shapes

[C. F. Berger, T. Kucs and G. F. Sterman' 2003]

$$\tau_a = \frac{2}{Q} \sum_{i \in \mathcal{X}} |\mathbf{p}_\perp^i| \, e^{-|\eta_i|(1-a)}$$

Depends on continuous parameter

$$\eta = \frac{1}{2} \ln\left(\frac{p^-}{p^+}\right)$$

A more general event shape!

provide access from thrust to jet broadening in continuous manner

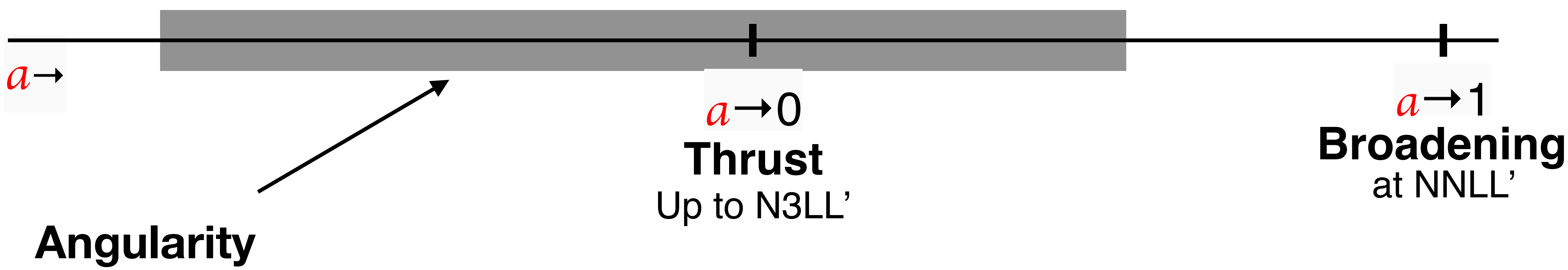

For e^+e^- = dijet

$$\tau_a^{ee} = \frac{2}{Q^2} \sum_{i \in \chi} min\left\{(p_i.n)^{a/2}(p_i.\bar{n})^{(1-a/2)}\right\}$$

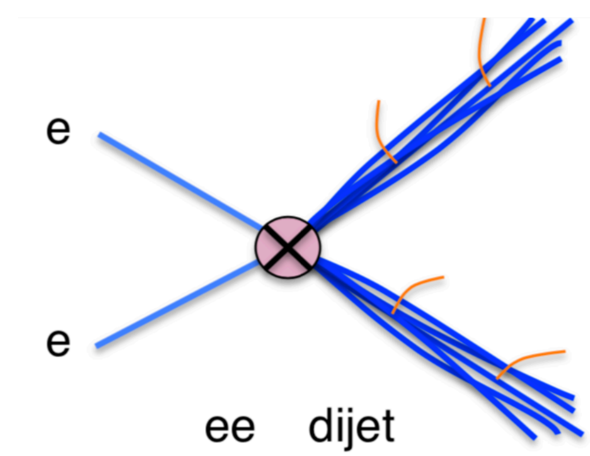

$$n.\bar{n} = 2$$

Global event shapes **Status**

Expt.

e+e-:
LEP: [P. Achard *et al.*, JHEP 1110, 143 (2011)]

DIS angularity at EIC!!

e+e- : **LEP:** [P. Achard *et al.*, JHEP 1110, 143 (2011)]

DIS: HERA by the ZEUS and H1 collaborations :

[1] C. Adloff *et al.* [H1], Phys. Lett. B 406, 256 (1997)
[2] C. Adloff *et al.* [H1], Eur. Phys. J. C 14, 255 (2000)
[3] A. Aktas *et al.* [H1], Eur. Phys. J. C 46, 343 (2006)
[4] J. Breitweg *et al.* [ZEUS], Phys. Lett. B 421, 368 (1998)
[5] S. Chekanov *et al.* [ZEUS], Eur. Phys. J. C 27, 531 (2003)
[6] S. Chekanov *et al.* [ZEUS], Nucl. Phys. B 767, 1 (2007)

$a \rightarrow$

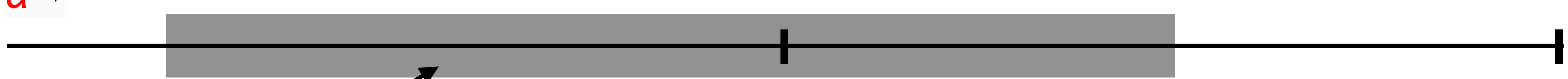

$a \rightarrow -2$

Angularity

$a \rightarrow 0$
Thrust
Up to N3LL'

$a \rightarrow 1$
Broadening
at NNLL'

SCET

e+e- : Hornig, Lee, Ovanesyan'09; Bell, Hornig, Lee, Talbert'18, A.Budhraja, A.Jain and M.Procura'19

Photoproduction:
E.C.Aschenauer, K.Lee, B.S.Page and F.Ringer'19

DIS angularity??

Tanmay Maji, D. Kang, J. Zhu, JHEP11(2021) 026

e+e- : Catani, Trentadue, Turnock, Webber'93; Florian, Grazzini'04; Schwartz'07; Becher, Schwartz'08; Abbate, Fickinger, Hoang, Mateu, Stewart'10 ;Becher,Schwartz'08; Stewart,Tackmann,Waalewijn'10 …

pp : Stewart,Tackmann,PRL'10,'11;PRD'13

DIS: D. Kang,C. Lee,I. Stewart'13

Dokshitzer, Lucenti, Marchesini, Salam'98; Becher, Bell, Neubert'11; Chiu, Jain, Neill, Rothstein'11; Becher and Bell'12

Why DIS angularity?

Puzzle in Strong Coupling determination

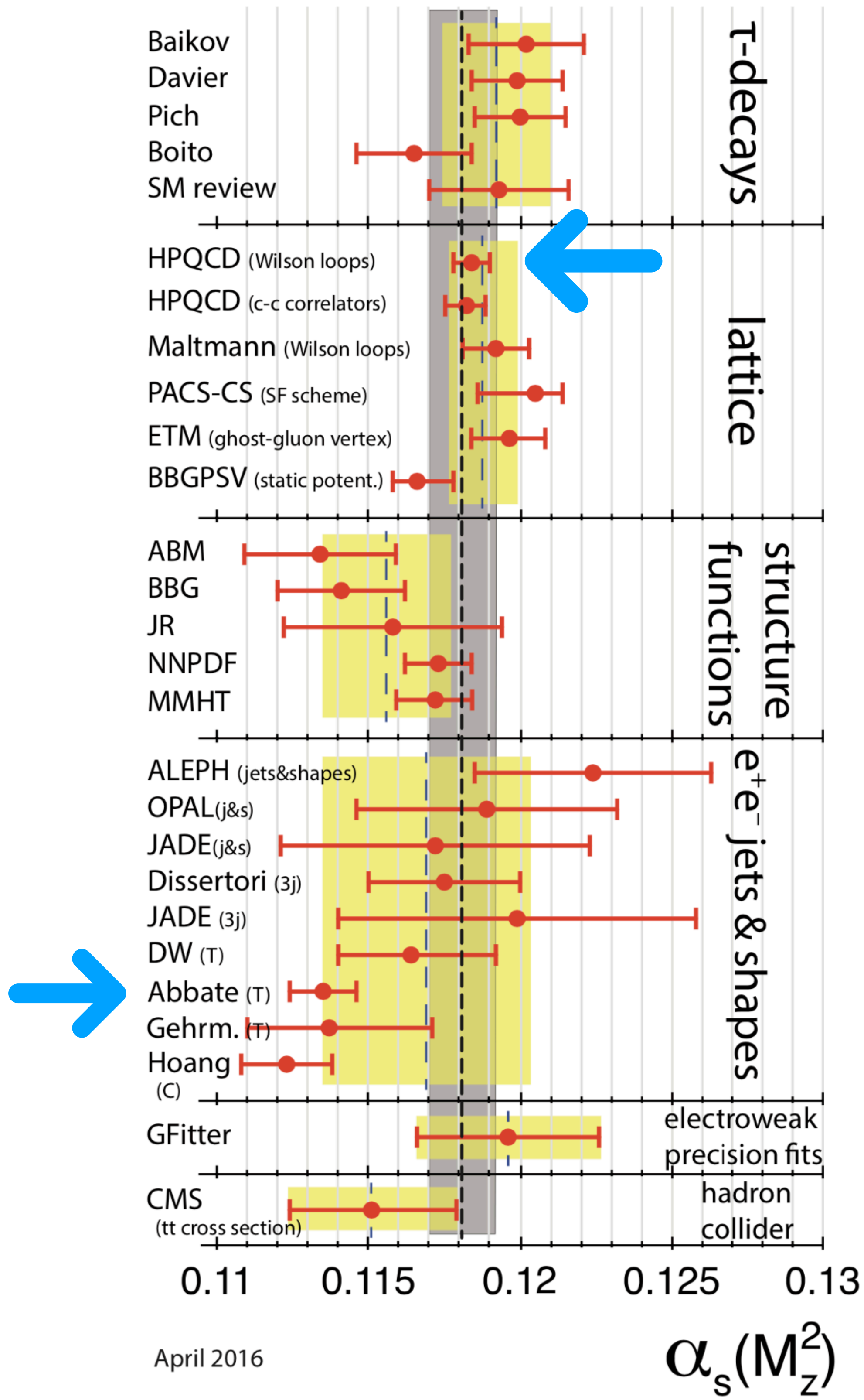

Discrepancy> 3-Sigma from Lattice

Need a new test from an independent experiment and new event shapes!

Why DIS angularity?

- Shed lights on the puzzle in strong coupling constant determination
- DIS event shapes for **future Electron-Ion-Collider (EIC)** at BNL!!

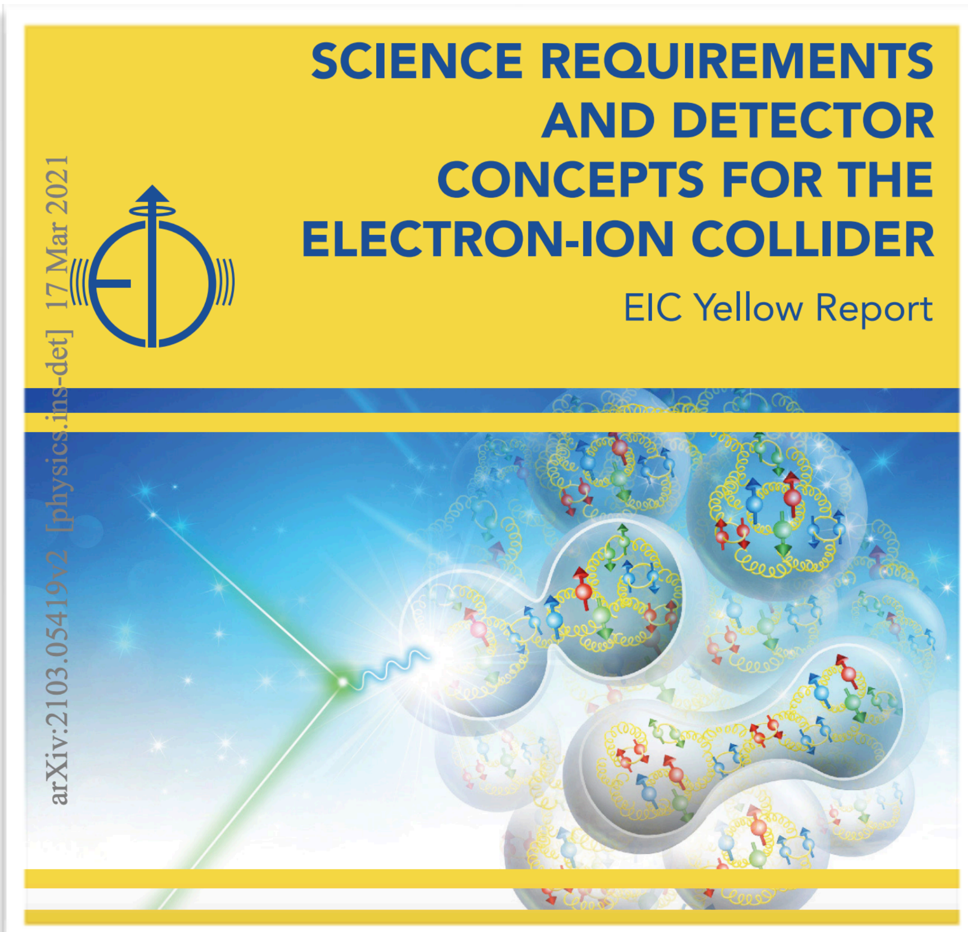

process, although acceptance up to higher rapidity (for example, $\eta = 4.5$) would provide a longer lever arm allowing for more stringent tests of the small-x dynamics and the Pomeron. Apart from J/ψ production, the rapidity-gap production of ρ-mesons maybe also very promising, perhaps even over a broader $|t|$-range.

7.1.7 Global event shapes and the strong coupling constant

Introduction

Event shapes [289] are global measures of the momentum distribution of hadrons in the final state of a collision, using a single number to characterize how well collimated the hadrons are along certain axes. This simple and global nature makes them highly amenable to high-precision theoretical calculations and convenient for experimental measurements. They then become powerful probes of QCD predictions, the strong coupling α_s, hadronization effects, etc.

The classic example, for collisions $e^+e^- \to X$, is *thrust* [290,291],

$$\tau = 1 - T, \quad \text{where} \quad T = \frac{1}{Q}\max_{\hat{t}} \sum_{i\in X} |\hat{\boldsymbol{t}} \cdot \boldsymbol{p}_i| = \frac{2}{Q} p_z^A, \tag{7.13}$$

at a center-of-mass collision energy Q, summing the three-momenta $\boldsymbol{p}_i$ of all final-state hadrons $i \in X$ projected onto the thrust axis $\hat{\boldsymbol{t}}$, which is defined as the axis maximizing the sum. It is customary to use $\tau = 1 - T$, whose $\tau \to 0$ limit describes pencil-like back-to-back two-jet events, and which grows as the jets broaden, up to the limit $\tau = 1/2$ for a spherically symmetric final state. Other examples of two-jet event shapes in e^+e^- are broadening B [292], C-parameter [293], and angularities [294,295].

Could be an early milestone!

Angularity
in the deep-inelastic scattering!

$$e(l) + N(P) \to e(l') + \text{dijet}$$

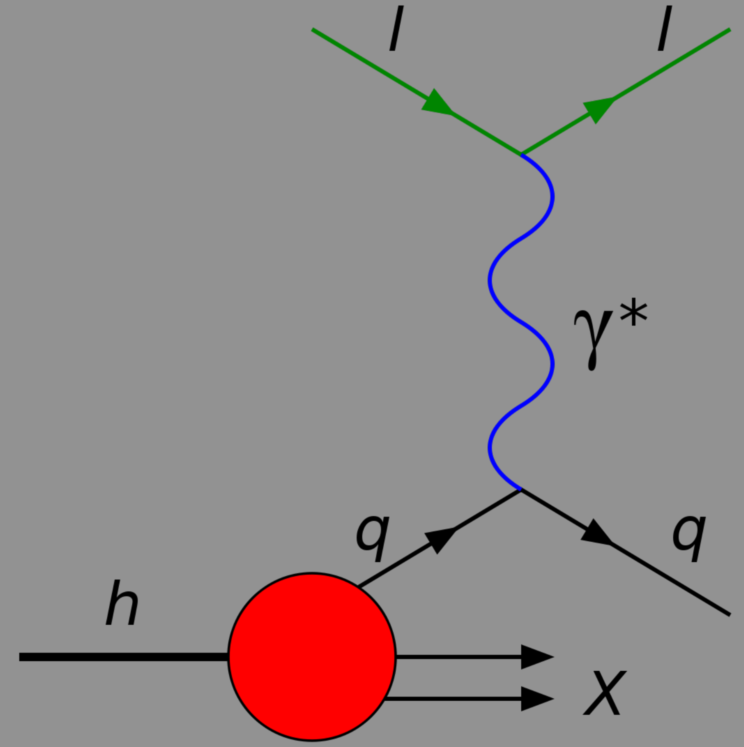

Angularity for DIS

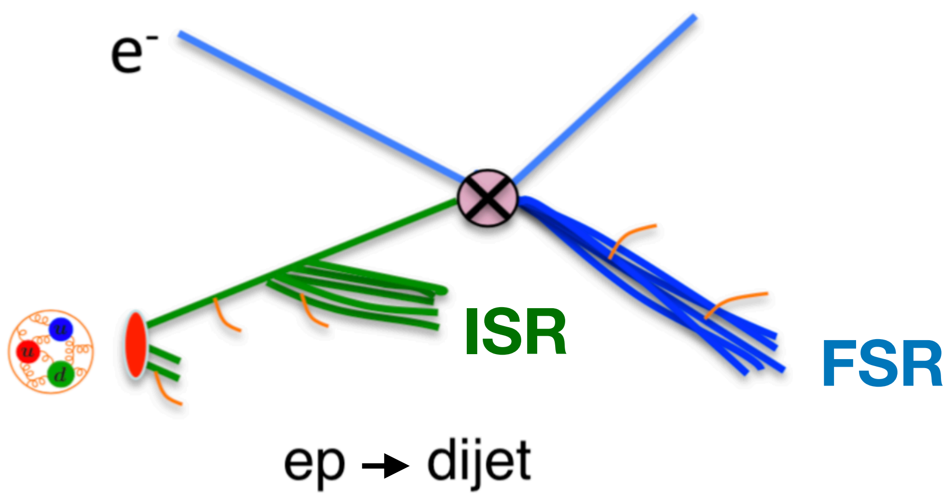

Not back to back even in CM !!

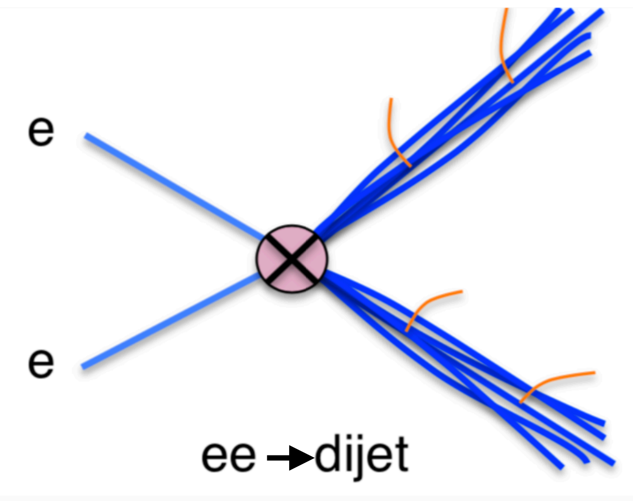

Back to back in CM frame

$$n.\bar{n} = 2$$

Angularity for DIS

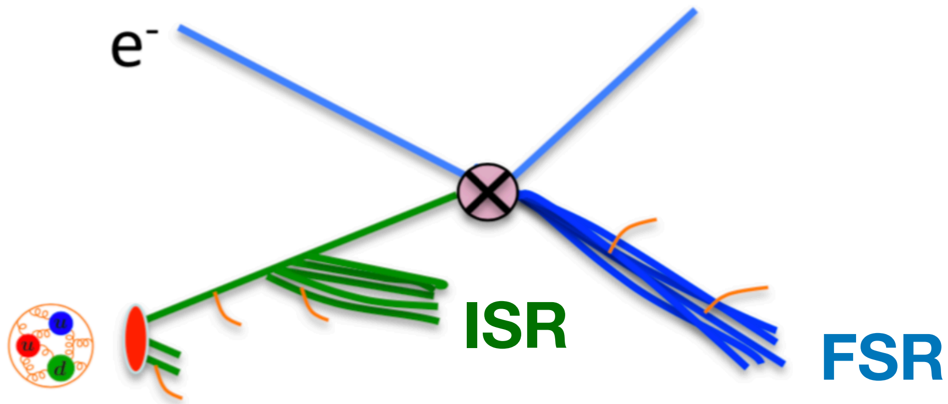

Not back to back even in CM !!

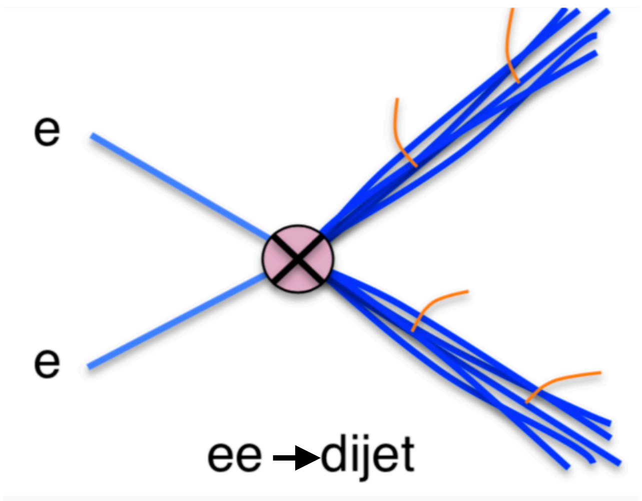

Back to back in CM frame

$$n.\bar{n} = 2$$

Axis Choice: qB = xP, qJ= jet axis

$$q_B^\mu = \omega_B \frac{n_B^\mu}{2} \quad \text{and} \quad q_J^\mu = \omega_J \frac{n_J^\mu}{2} \quad \text{with} \quad \boxed{n_i \cdot \bar{n}_i = 2}$$

$$\text{we obtain } \omega_B = \bar{n}_B \cdot q_B \text{ and } \omega_J = \bar{n}_J \cdot q_J$$

$$\boxed{\tau_a = \frac{2}{Q^2} \sum_{i \varepsilon \mathscr{X}} min\left\{ (q_B.p_i) \left(\frac{q_B.p_i}{q_J.p_i} \right)^{-a/2}, (q_J.p_i) \left(\frac{q_J.p_i}{q_B.p_i} \right)^{-a/2} \right\}}$$

Angularity diff. cross-section for DIS

$$\frac{d\sigma}{dx\,dQ^2\,d\tau_a} = L_{\mu\nu}(x, Q^2)\; W^{\mu\nu}(x, Q^2, \tau_a)$$

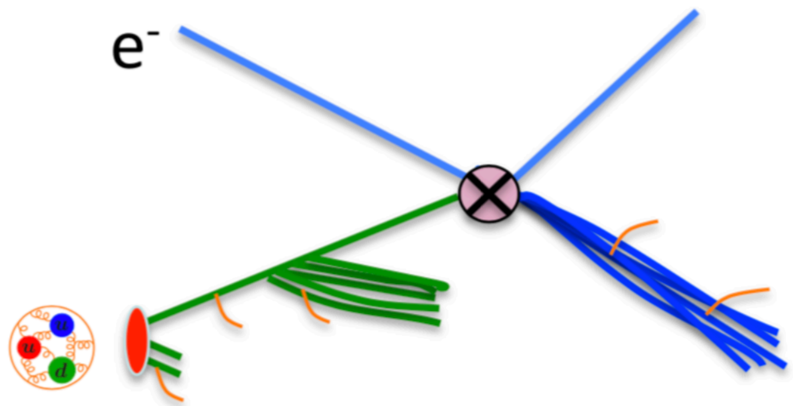

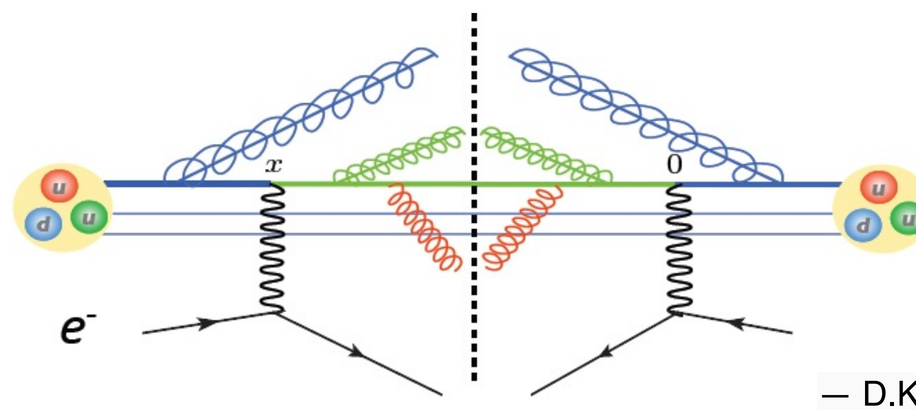

— D.Kang,Lee,Stewart'2013
Z.Kang,Mantry,Qiu'2012

$$\boxed{\begin{aligned}\frac{d\sigma}{dx\,dQ^2\,d\tau_a} &= \frac{d\sigma_0}{dx\,dQ^2}\int d\tau_a^J\, d\tau_a^B\, d\tau_a^S\, \delta\Big(\tau_a - \tau_a^J - \tau_a^B - \tau_a^S\Big) \\ &\quad \times \sum_{i=q,\bar q} H_i(Q^2,\mu)\, \mathcal{B}_i(\tau_a^B, x, \mu)\, J(\tau_a^J,\mu)\, S(\tau_a^S,\mu)\end{aligned}}$$

Power counting in SCET

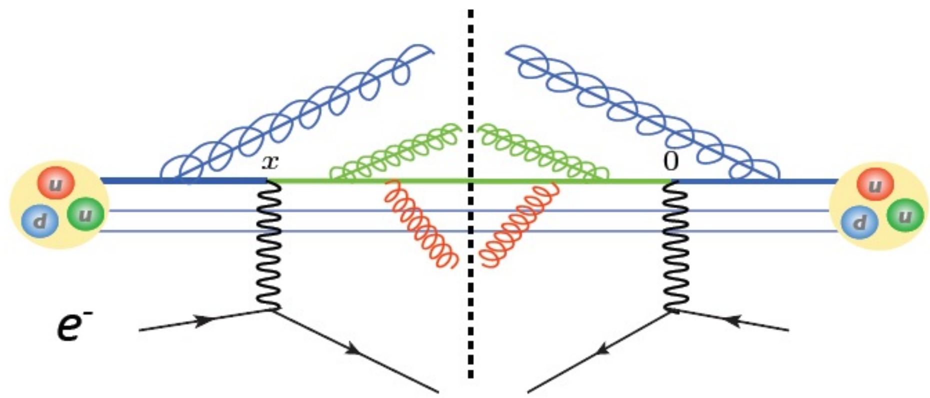

$$p = p^+ \frac{\bar{n}_B}{2} + p^- \frac{n_B}{2} + p_\perp$$

Collinear and soft modes

$$p_c \sim Q(\lambda_c^2, 1, \lambda_c)\,, \qquad \tau_a^B(p_c) \sim \lambda_c^{2-a}$$
$$p_s \sim Q(\lambda_s, \lambda_s, \lambda_s)\,, \qquad \tau_a^B(p_s) \sim \lambda_s$$

This implies relevant soft mode contributing to τ_a^B has a scale of

$$\lambda_s \sim \lambda_c^{2-a}\,.$$

Soft and collinear splitting

$$p_c^2 \sim Q^2 \lambda^{2-a} \qquad p_s^2 \sim Q^2 \lambda^{2(2-a)}$$

$p_\perp = 0$ plane

$p^2 = p^+ p^-$

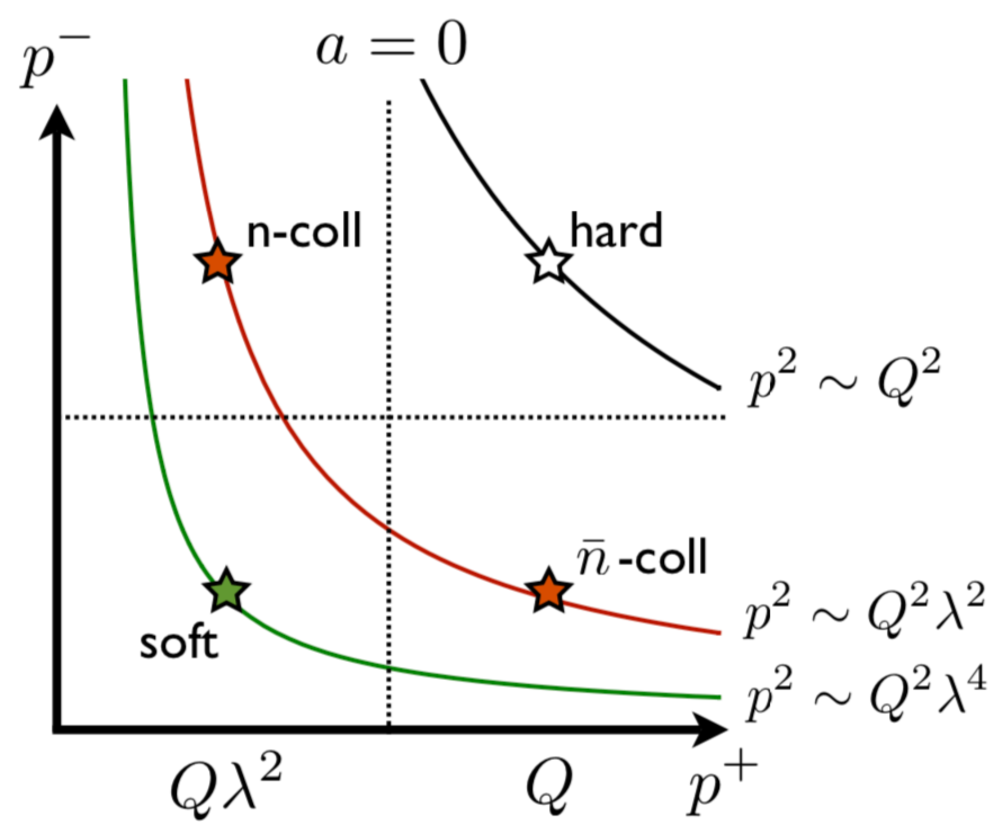

SCET facto.: dσ = Hard × Beam ⊗ Jet ⊗ Soft

Soft and collinear splitting

$$\frac{d\sigma}{dx dQ^2 d\tau_a} = \frac{d\sigma_0}{dx dQ^2} \int d\tau_a^J \, d\tau_a^B \, d\tau_a^S \, \delta\Big(\tau_a - \tau_a^J - \tau_a^B - \tau_a^S\Big)$$
$$\times \sum_{i=q,\bar{q}} H_i(Q^2,\mu)\mathcal{B}_i(\tau_a^B, x, \mu) J(\tau_a^J,\mu) S(\tau_a^S,\mu)$$

—Hornig, Lee, Ovanesyan'09;
—Bell, Hornig, Lee, Talbert'18,

Beam func.: $B(\tau_a, x, \mu) \;=\; \mathrm{pdf} \otimes \left[\delta_{qj}\delta(\tau_a) + \tilde{\mathcal{I}}_{qj}^{(1)} + \mathcal{O}(\alpha_s^2) + \ldots\right]$

$NP \qquad LO \qquad NLO \qquad NNLO$

$$\tilde{\mathcal{I}}_{qj}^{(1)} = \frac{\alpha_s}{4\pi}\left[\left(-j_B\kappa_B\frac{\Gamma_0}{2}L_B^2 - \gamma_0^B L_B\right)\mathbb{1}_{qj} + 4C_{qj}P_{qj}(z)L_B + \tilde{c}_1^{qj}(z,a)\right]$$

We present the angularity Beam function at one-loop

—Tanmay Maji, D. Kang, J. Zhu, JHEP11(2021) 026

Resummation in Laplace space

$$\frac{d\sigma}{dx dQ^2 d\tau_a} = \frac{d\sigma_0}{dx dQ^2} \int d\tau_a^J \, d\tau_a^B \, d\tau_a^S \, \delta\Big(\tau_a - \tau_a^J - \tau_a^B - \tau_a^S\Big)$$
$$\times \sum_{i=q,\bar{q}} H_i(Q^2,\mu) \mathcal{B}_i(\tau_a^B, x, \mu) J(\tau_a^J, \mu) S(\tau_a^S, \mu)$$

$$G(\nu,\mu) = \int_0^\infty d\tau_a e^{-\nu\tau_a} G(\tau_a,\mu)$$

$$\widetilde{\sigma}_q(\nu) = H_q(Q^2,\mu) \widetilde{\mathcal{B}}_q(\nu,\mu) \widetilde{J}(\nu,\mu) \widetilde{S}(\nu,\mu)$$

Resummation of large logs

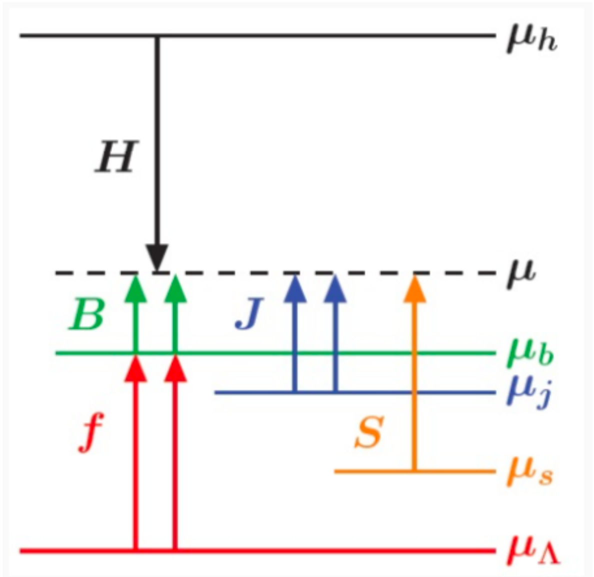

$$\mu_H = Q, \;\; \mu_{J,B} = Q\tau_a^{1/(2-a)}, \;\; \mu_S = Q\tau_a$$

	$\Gamma(\alpha_s)$	$\gamma(\alpha_s)$	$\beta(\alpha_s)$	$\{H,J,B,S\}[\alpha_s]$
LL	α_s	1	α_s	1
NLL	α_s^2	α_s	α_s^2	1
NNLL	α_s^3	α_s^2	α_s^3	α_s

Resummation of large logs

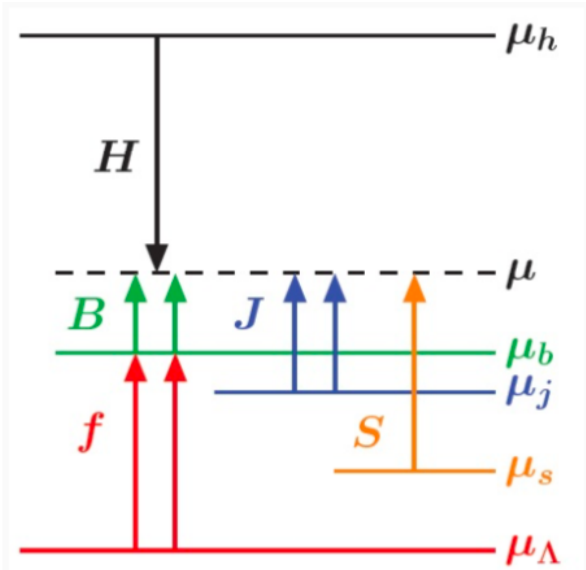

	$\Gamma(\alpha_s)$	$\gamma(\alpha_s)$	$\beta(\alpha_s)$	$\{H, J, B, S\}[\alpha_s]$
LL	α_s	1	α_s	1
NLL	α_s^2	α_s	α_s^2	1
NNLL	α_s^3	α_s^2	α_s^3	α_s

$$\mu_H = Q, \quad \mu_{J,B} = Q\tau_a^{1/(2-a)}, \quad \mu_S = Q\tau_a$$

Evolution Equation for beam function

$$\mu \frac{d}{d\mu} B(\nu,\mu) = \gamma_G(\mu)\, B(\nu,\mu) \;; \qquad \text{similar to} J, S, H$$

$$\text{Solution}: \; B(\nu,\mu) = B(\nu,\mu_B)\, e^{K_B(\mu_B,\mu) + j_B \eta_B(\mu_B,\mu) L_B},$$

- Jet and beam functions are defined by same collinear operator: $\gamma_J(\mu) = \gamma_B(\mu)$

$$K_B(\mu_B,\mu) = \underbrace{L_B \sum_{k=1}^{\infty} (\alpha_s L_B)^k}_{LL} + \underbrace{\sum_{k=1}^{\infty} (\alpha_s L_B)^k}_{NLL} + \ldots$$

$\boxed{\alpha_s L_B \sim 1}$

$L_B = \ln(\mu/\mu_B)$

LL: Leading Log;
NLL: Next-to-Leading Log

Large logs at threshold limit & Resummation

$$G^{\text{fixed}}(L_G,\mu) = 1 + \frac{\alpha_s(\mu)}{4\pi}\left[-j_G\kappa_G\frac{\Gamma_0}{2}L_G^2 - \gamma_0^G L_G + c_1^G\right], \qquad G=\{H,\widetilde{S},\widetilde{J}\}$$

$$L_G(\tau_a) = \ln\left[\frac{Q}{\mu_G}\left(\tau_a e^{-\gamma_E}\right)^{1/j_G}\right], \qquad G=\{S,J\}$$

With jB = 2-a

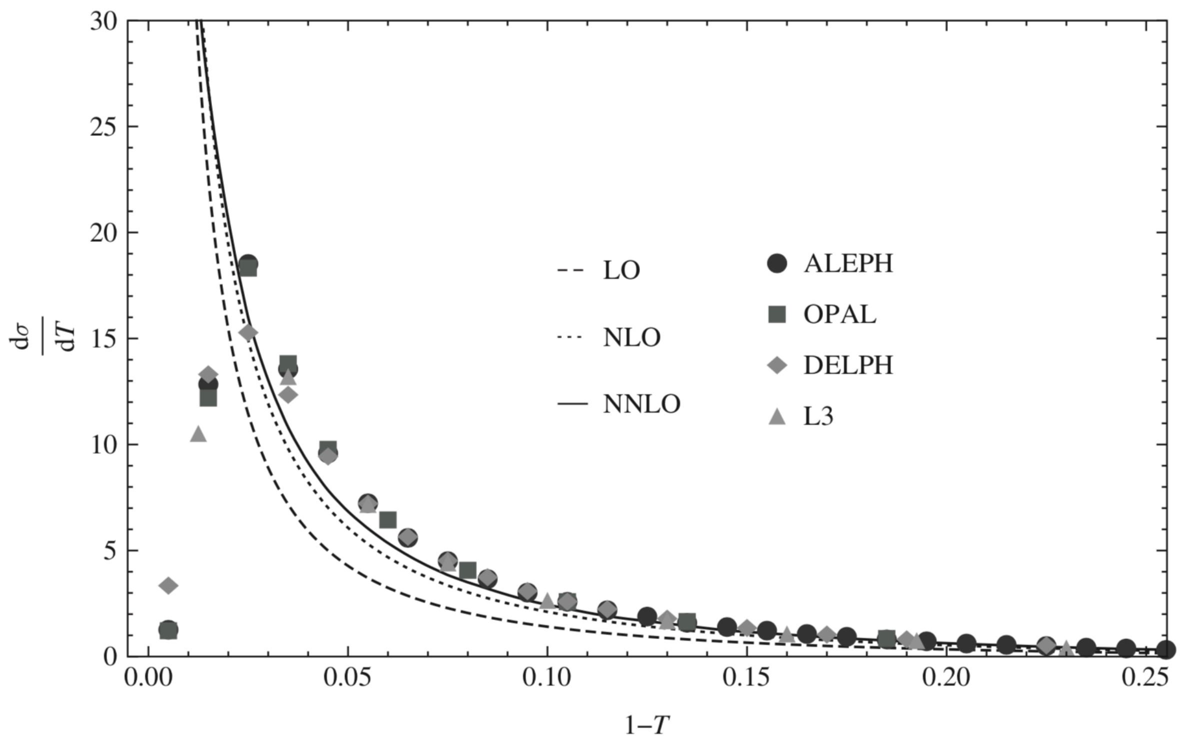

$$\begin{aligned}
\sigma = \sigma^{(0)} &\quad \text{leading order (LO)}\\
+\alpha_s\sigma^{(1)} &\quad \text{next-to-leading order (NLO)}\\
+\alpha_s^2\sigma^{(2)} &\quad \text{next-next-to-leading order (NNLO)}\\
+\cdots &
\end{aligned}$$

Large logs at threshold limit & Resummation

$$G^{\text{fixed}}(L_G,\mu) = 1 + \frac{\alpha_s(\mu)}{4\pi}\left[-j_G\kappa_G\frac{\Gamma_0}{2}L_G^2 - \gamma_0^G L_G + c_1^G\right], \qquad G = \{H, \widetilde{S}, \widetilde{J}\}$$

$$L_G(\tau_a) = \ln\left[\frac{Q}{\mu_G}\left(\tau_a e^{-\gamma_E}\right)^{1/j_G}\right], \qquad G = \{S, J\}$$

With jB = 2-a

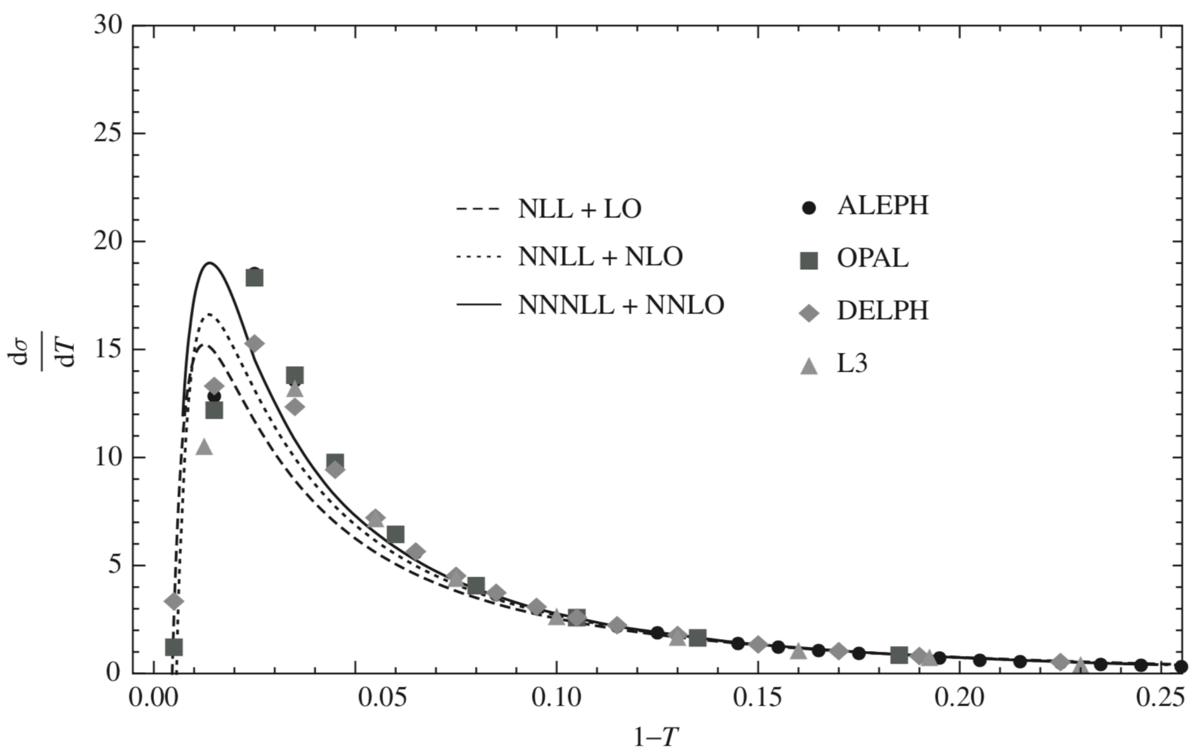

$$\begin{aligned}\sigma = \sigma^{(0)} & \quad \text{leading order (LO)} \\ + \alpha_s\sigma^{(1)} & \quad \text{next-to-leading order (NLO)} \\ + \alpha_s^2\sigma^{(2)} & \quad \text{next-next-to-leading order (NNLO)} \\ + \cdots & \end{aligned}$$

$$K_B(\mu_B,\mu) = L_B\sum_{k=1}^{\infty}(\alpha_s L_B)^k$$

Leading Log (**LL**)

$$+\sum_{k=1}^{\infty}(\alpha_s L_B)^k$$

Next-to-leading Log (**NLL**)

$$+ \ldots$$

Next-to-next-leading Log (**NNLL**)

Results

DIS Angularity Beam function $B(\tau_a^B, x, \mu)$

DIS Angularity Differential Cross-section $\dfrac{d\sigma^{DIS}}{dx dQ^2 d\tau_a} = ?$

Angularity Beam function at NNLL accuracy

Beam func.: $B(\tau_a, x, \mu) = \text{pdf} \otimes \left[\delta_{qj}\delta(\tau_a) + \tilde{\mathcal{I}}^{(1)}_{qj} + \mathcal{O}(\alpha_s^2) + \ldots\right]$

$NP \quad LO \quad NLO \quad NNLO$

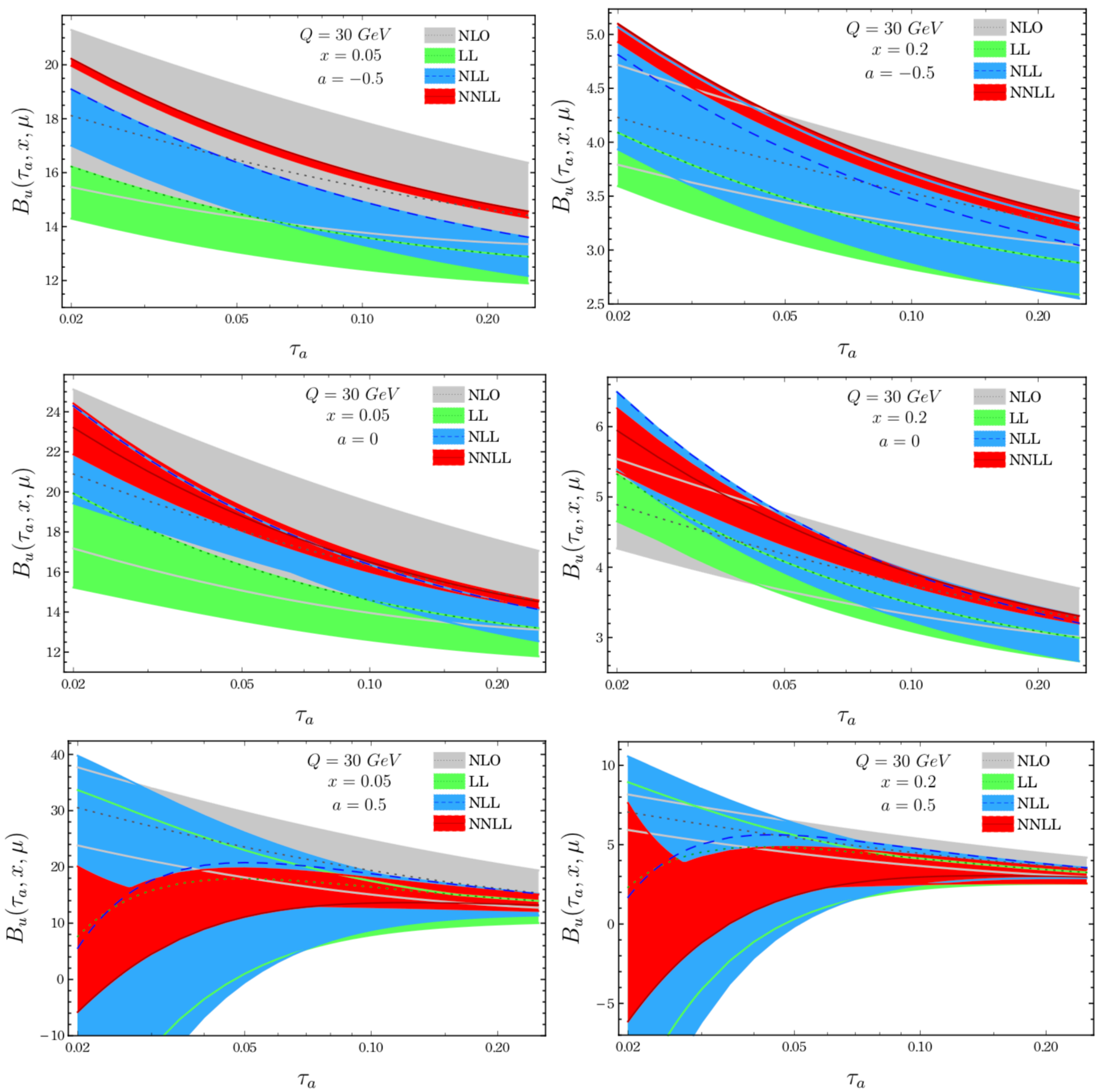

<- a= - 0.5

<- Thrust limit

<- a= 0.5

Resummation of large logs provides better perturbative convergence.

Angularity Differential Cross-section

$$\frac{d\sigma}{dx\,dQ^2 d\,\tau_a} = \frac{d\sigma_0}{dxdQ^2} \sum_\nu H_\nu(Q^2,\mu) \int d\tau_a^J\, d\tau_a^B\, dk_S\, J_q(\tau_a^J,\mu) B_{\nu/q}(\tau_a^B,x,\mu)$$
$$\times S(k_S,\mu)\delta\left(\tau_a - \tau_a^J - \tau_a^B - \frac{k_S}{Q_R}\right),$$

Angularity Differential Cross-section

$$\frac{d\sigma}{dx\,dQ^2 d\,\tau_a} = \frac{d\sigma_0}{dxdQ^2}\sum_\nu H_\nu(Q^2,\mu)\int d\tau_a^J\,d\tau_a^B\,dk_S\,J_q(\tau_a^J,\mu)B_{\nu/q}(\tau_a^B,x,\mu)$$
$$\times S(k_S,\mu)\delta\left(\tau_a-\tau_a^J-\tau_a^B-\frac{k_S}{Q_R}\right),$$

Resummed result

$$\begin{aligned}
\sigma(x,Q^2,\tau_a,\mu) \quad &= \quad \sigma_0(x,Q^2)\left(\frac{Q}{\mu_H}\right)^{\eta_H(\mu,\mu_H)} e^{\kappa(\mu_H,\mu_J,\mu_B,\mu_S,\mu)} \\
&\times\left(\left(\frac{Q}{\mu_J}\right)^{2-a}\tau_a e^{-\gamma_E}\right)^{\eta_J(\mu,\mu_J)}\left(\left(\frac{Q}{\mu_B}\right)^{2-a}\tau_a e^{-\gamma_E}\right)^{\eta_B(\mu,\mu_B)}\left(\frac{Q^2}{\mu_S}\tau_a e^{-\gamma_E}\right)^{2\eta_S(\mu,\mu_S)} \\
&\times\tilde{j}_q\left(\partial_\Omega+\log\left(\frac{Q^{2-a}}{\mu_J^{2-a}}\tau_a e^{-\gamma_E}\right),\mu_J\right)\tilde{s}\left(\frac{1}{Q_R}\left(\partial_\Omega+\log(\frac{Q}{\mu_S}\tau_a e^{-\gamma_E})\right),\mu_S\right) \\
&\times\left[H_q(y,Q^2,\mu_H)\tilde{b}_q\left(\partial_\Omega+\log\left(\frac{Q^{2-a}}{\mu_B^{2-a}}\tau_a e^{-\gamma_E}\right),x,\mu_B\right)\right. \\
&\left.+H_{\bar{q}}(y,Q^2,\mu_H)\tilde{b}_{\bar{q}}\left(\partial_\Omega+\log\left(\frac{Q^{2-a}}{\mu_B^{2-a}}\tau_a e^{-\gamma_E}\right),x,\mu_B\right)\right]\frac{1}{\tau_a\Gamma(\Omega)}
\end{aligned}$$

Numerical results at NNLL

- DIS angularity cross-section at NNLL accuracy

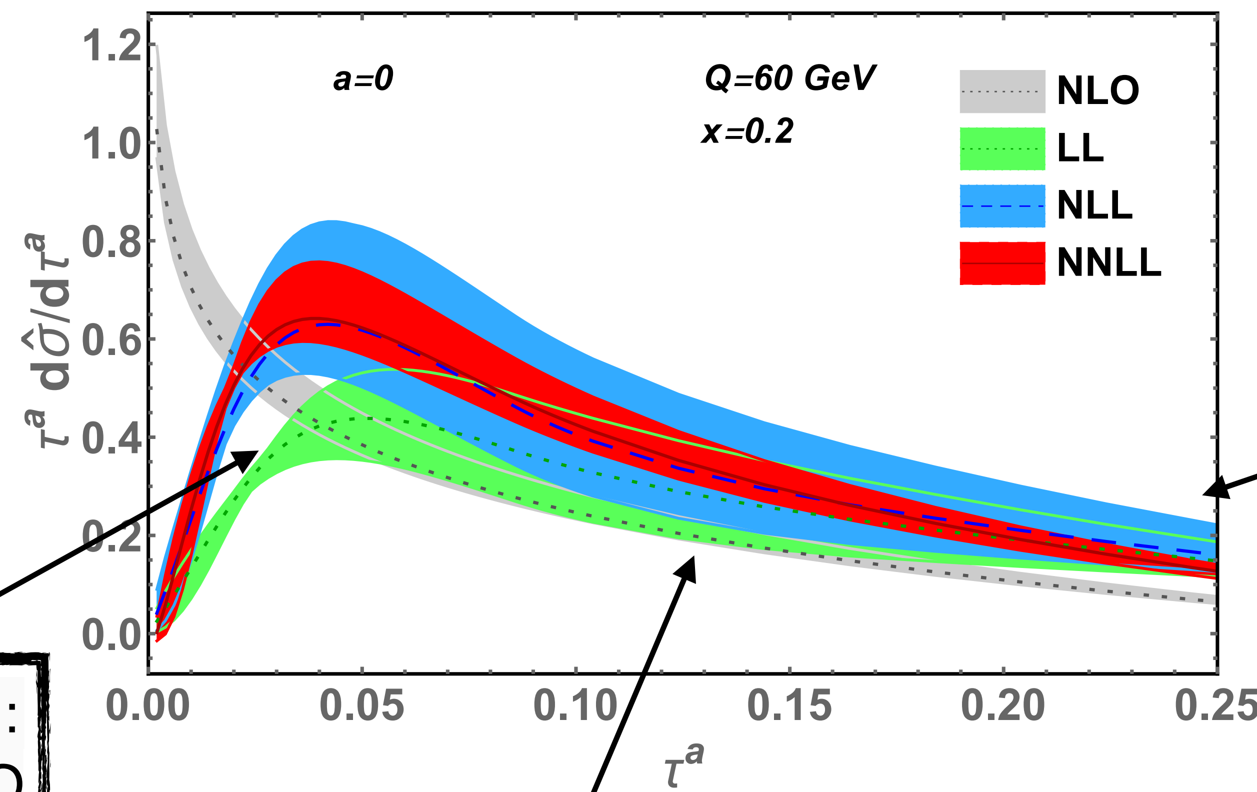

Far-tail region: Need full QCD

Low angularity region: Log singularity at NLO

Tail region:

Resummation gives convergence from LL to NNLL

Relative Uncertainty

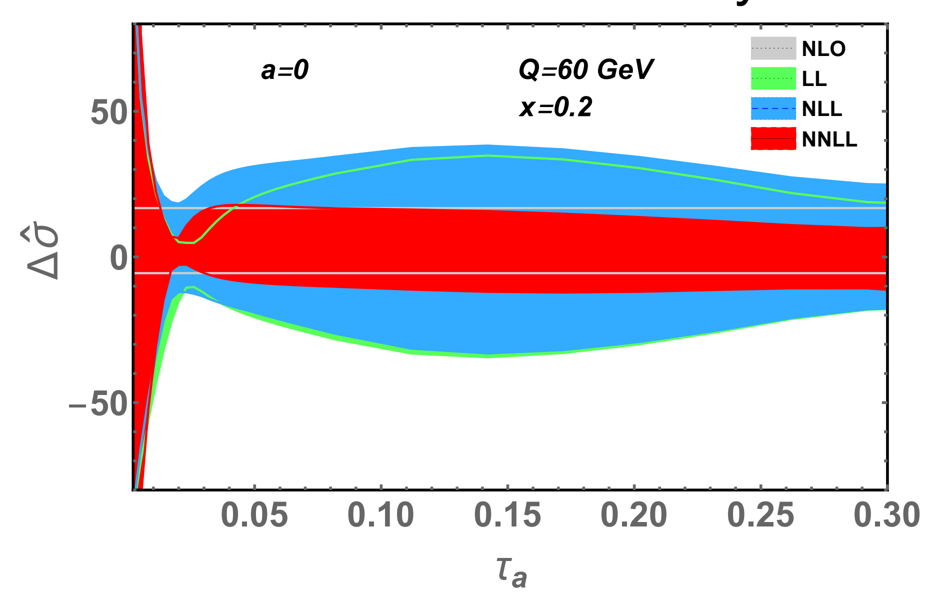

‘a’ dependency

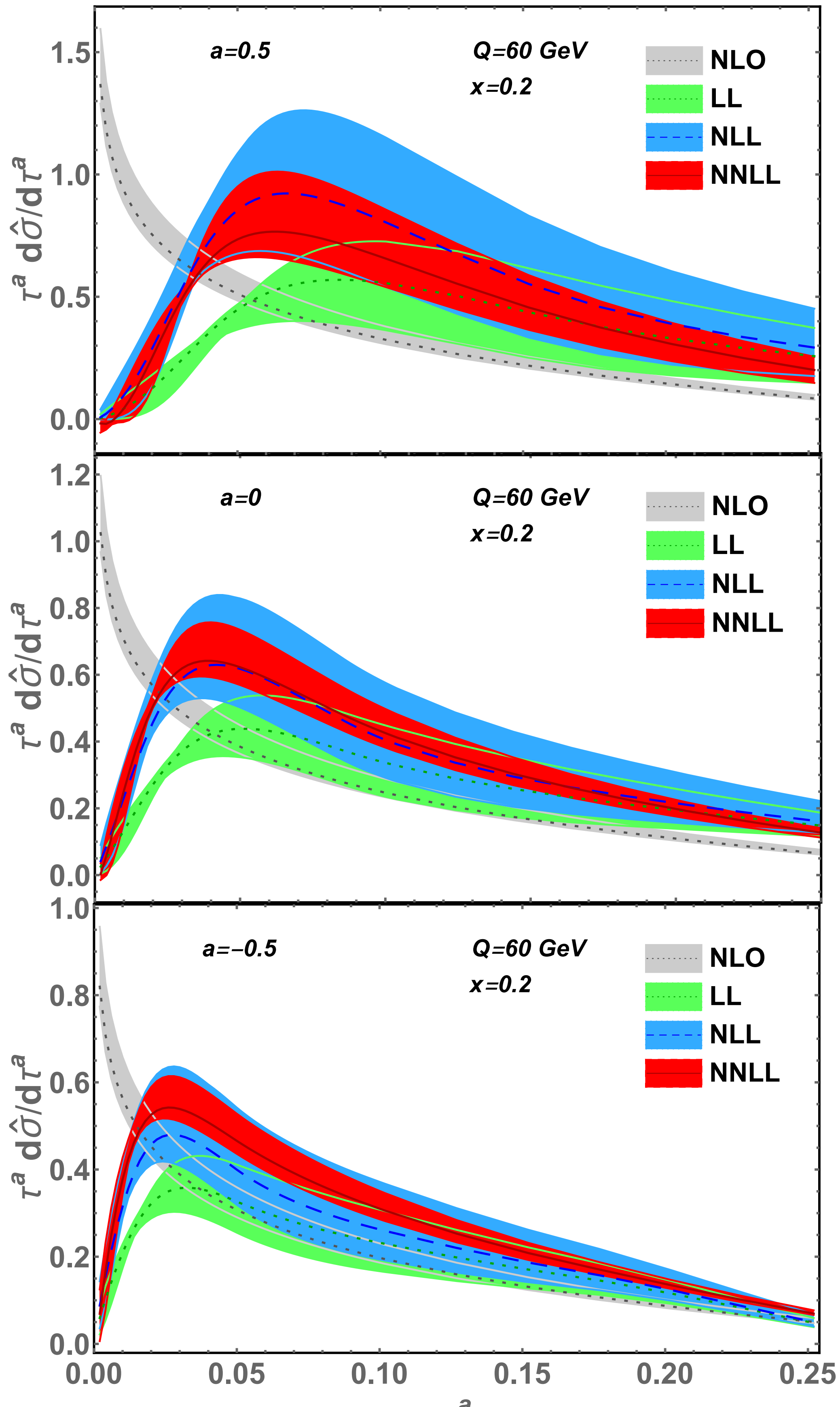

Relative uncertainty at NNLL

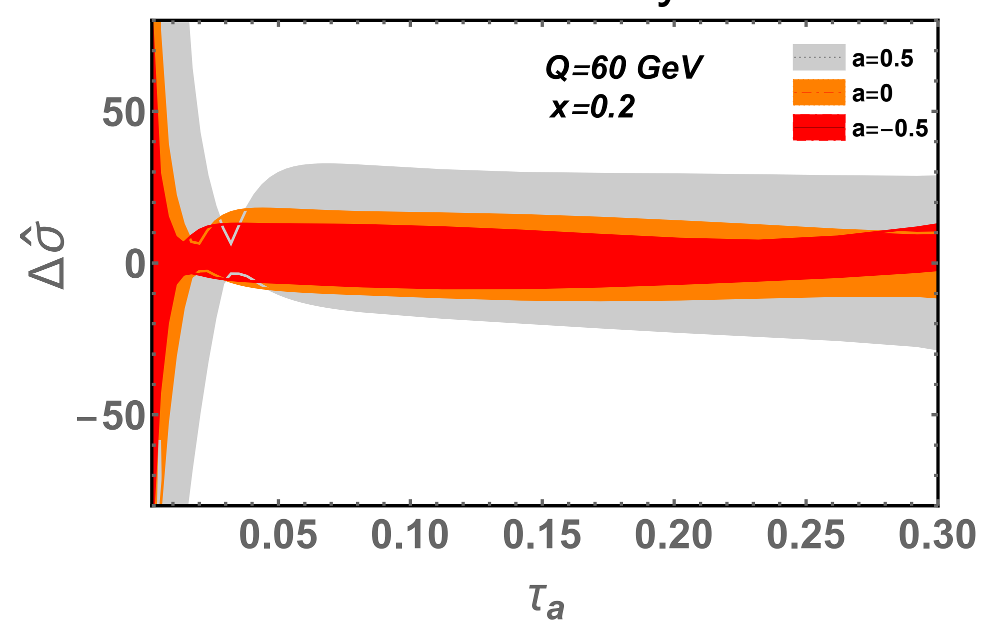

- Uncertainty in DIS angularity cross-section is sensitive to the angularity parameter ‘a’.
- Prediction is more precise for negative ‘a’

‘x’ dependency

Relative uncertainty at NNLL

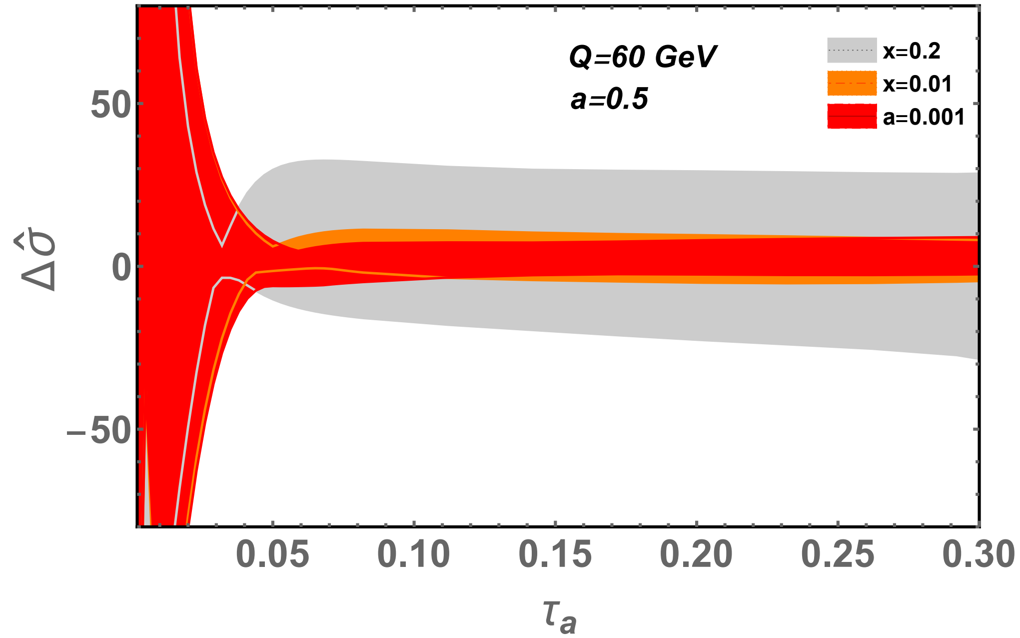

- Uncertainty in the angularity cross-section depends on the longitudinal momentum fraction (x) of the partons.
- Prediction is more precise for the region x going small

uncertainty depends on the angularity parameter ‘a’ as well as on the longitudinal mo mentum fraction ‘x’ of the partons.

Prediction is more precise for small-‘x’ and negative ‘a’ region.

Beam Func. & Fragmentation func.

Beam at NLO: $i \to k^* j$

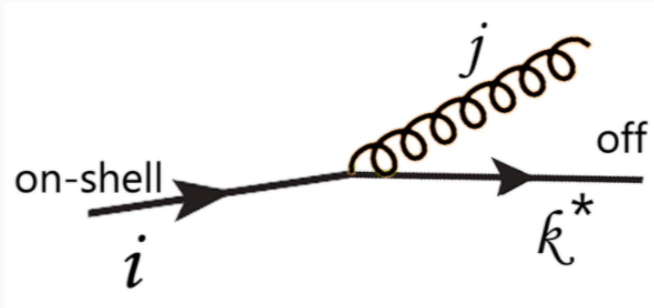

Crossing Symmetry!

Fragmentation at NLO: $i^* \to kj$

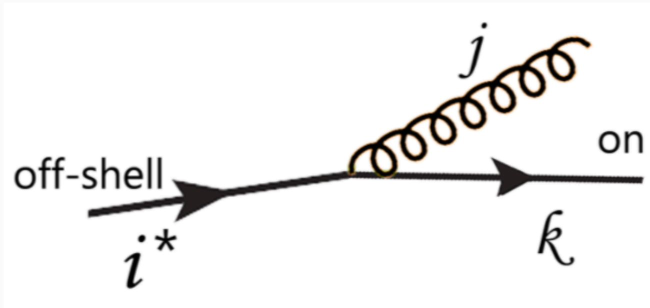

Splitting Function: [M.Ritzmann,W.J.Waalewijn,PRD90(2014)]

$$P_{i \to k^* j}(2pi.pj, x) \equiv (-1)^{\Delta_f} P_{k* \to ij}(-2pi.pj, 1/x)$$

- Change comes only from the two-particle phase-space and effectively change in sign of the $\log(x)$ term in the matching co-efficient $\mathcal{I}^{(1)}$.

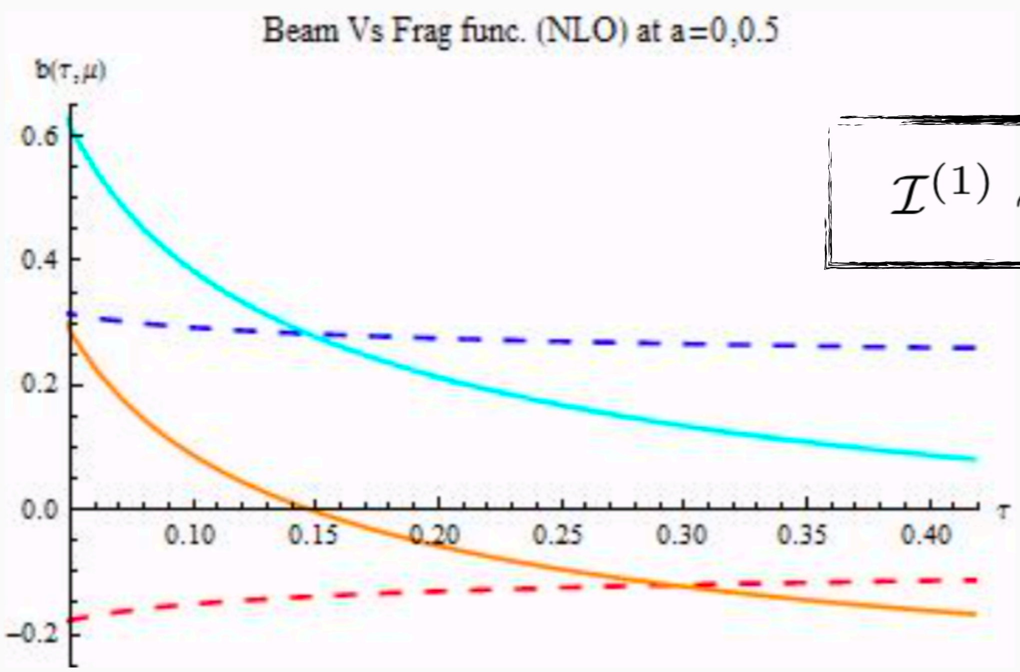

$$\boxed{\mathcal{I}^{(1)} \sim \ldots - \frac{\alpha_s C_F}{2\pi} \frac{2(1-a)}{2-a} \frac{1+x^2}{1-x} \log x}$$

Beam match. Coeffi.: $a = 0$
Beam match. Coeffi.: $a = 0.5$

FF match. Coeffi.: $a = 0$
FF match. Coeffi.: $a = 0.5$

- Difference decreases with the increase of angularity parameter a.

Angularity in H -> gg at NNLL’ accuracy

Angularity in Higgs Decay

Higgs decay into hadronic channels (bb, gg, cc,…)

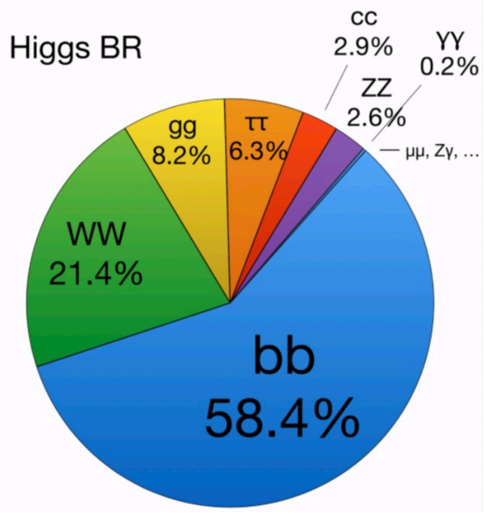

Current accuracy: Higgs -> qq at NNLL’

Higgs -> gg at NNLL

Goal: Higgs -> gg at NNLL’

	$\Gamma(\alpha_s)$	$\gamma(\alpha_s)$	$\beta(\alpha_s)$	$\{H, J, B, S\}[\alpha_s]$
LL	α_s	1	α_s	1
NLL	α_s^2	α_s	α_s^2	1
NNLL	α_s^3	α_s^2	α_s^3	α_s
NNLL$'$	α_s^3	α_s^2	α_s^3	α_s^2

Higgs decay rate h -> gg (Fixed order)

$$\boxed{\begin{aligned}\frac{d\Gamma^i}{d\tau_a} = \Gamma_B^i(\mu)|C_t^i(m_t,\mu)|^2\,|C_S^i(m_H,\mu)|^2 \int d\tau_a^{J1}\,d\tau_a^{J2}d\tau_a^S\,\delta\Big(\tau_a-\tau_a^{J1}-\tau_a^{J2}-\tau_a^S\Big)\\ \times J^i(\tau_a^{J1},\mu)\,J^i(\tau_a^{J2},\mu)\,S^i(\tau_a^S,\mu)\,,\end{aligned}}$$

Born decay rates $\quad \Gamma_B^g(\mu) \;=\; \frac{m_H^3\alpha_s^2(\mu)}{72\pi^3 v^2}$

Wilson coefficient,
top loop coupled to two gluons $\quad C_t(m_t,\mu) = 1 + \sum_{n=1}^{\infty}\left(\frac{\alpha_s(\mu)}{4\pi}\right)^n C_t^{(n)}(m_t,\mu)$

[PRL, **118** (2017) 082002; PRL, **79** (1997) 353]

Hard coefficient $\quad C_S^i(m_H,\mu) = 1 + \sum_{n=1}^{\infty}\left(\frac{\alpha_s(\mu)}{4\pi}\right)^n C_S^{i(n)}(L_H)$

Cs is defined from the matching to SCET and can be obtained from Hqq and Hgg form factors that are available **up to the 3-loop.** [PRD **78** (2008) 034027; *JHEP* **07** (2008) 034; PRD **77** (2008) 014026; J*HEP* **06** (2010) 094]

Higgs decay rate h -> gg (Fixed order)

$$\boxed{\begin{aligned}\frac{d\Gamma^i}{d\tau_a} = \Gamma^i_B(\mu)|C^i_t(m_t,\mu)|^2\,|C^i_S(m_H,\mu)|^2 \int d\tau_a^{J1}\,d\tau_a^{J2}d\tau_a^S\,\delta\Big(\tau_a - \tau_a^{J1} - \tau_a^{J2} - \tau_a^S\Big)\\ \times J^i(\tau_a^{J1},\mu)\,J^i(\tau_a^{J2},\mu)\,S^i(\tau_a^S,\mu)\,,\end{aligned}}$$

☑ Angularity **soft functions** $S^i(\tau_a,\mu)$ describing soft emissions from light-like quark or gluon and is available up to **2-loop orders** for both the quarks and gluons.

[C. Lee, et. al. *JHEP* **05** (2009) 122; G. Bell et. al., *JHEP* **09** (2020) 015]

☑ The angularity **jet functions** $J^i(\tau_a, \mu)$ describe the collinear emission along the direction of initial quark or, gluon. **Quark angularity jet function is unto 2-loop and gluon angularity jet function is unto 1-loop** is calculated recently.

[C. Lee et. al., *JHEP* **05** (2009) 122; *JHEP* **01** (2019) 147]

We compute Gluon angularity jet function at 2-loop: The constant C^J_2 at 2-loop

[J. Zhu,J. Gao, D. kang, TM, arXiv:2311.07282v1]

In the determination of the constant, there is significant contamination from subleading singular corrections slowly suppressed in small τ_a limit. In order to estimate the correction, we use asymptotic forms in small τ_a region and fit it to the nonsingular part of fixed-order result.

Results: Angularity in Hgg at NNLL’

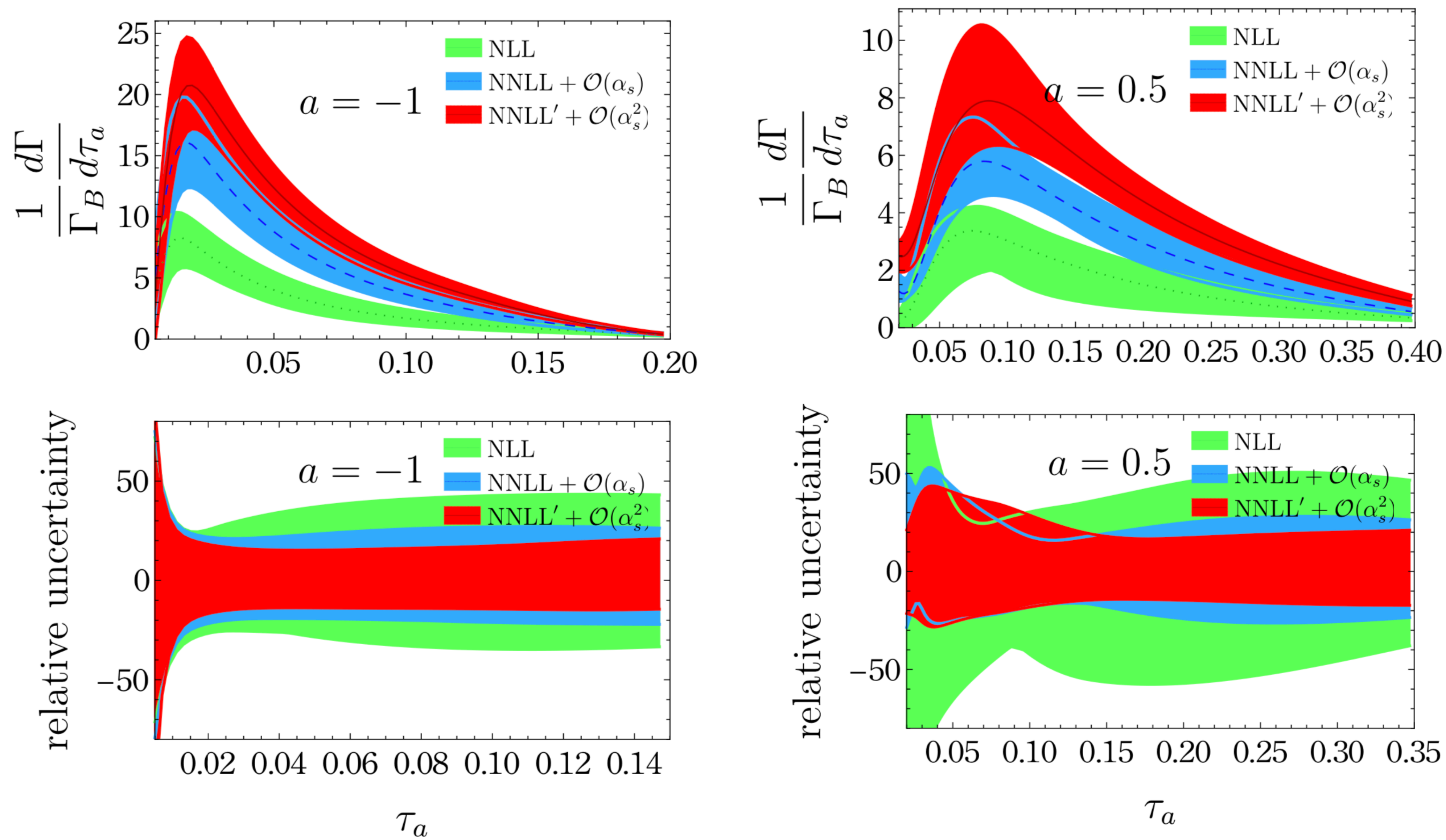

[J. Zhu,J. Gao, D. kang, TM, arXiv:2311.07282v1]

- Resummed distribution received large correction from higher order
- The uncertainty is more sensitive to the angularity perimeter a for the higher order
- For NNLL to NNLL’: Uncertainty is reduced by12% for a=-1 and by 5% for a=0.5

Summary and Conclusion

☑ **DIS Angularity:** Presented the one-loop angularity beam function precision prediction to the DIS angularity cross-section at NNLL accuracy.

uncertainty depends on the angularity parameter 'a' as well as on the longitudinal momentum fraction 'x' of the partons.

Prediction is more precise for negative 'a' and 'x' going small region.

This prediction could be considered as one of the early milestone to event shape measurement at EIC

☑ **Angularity Hgg:** We present improved predictions of angularity distribution τ_a in hadronic decays of Higgs boson via effective operator $H \to gg$ that suffers from large perturbative uncertainties on subleading NP corrections. The distribution is improved by resumming large logarithms of angularity at NNLL accuracy in the frame work of SCET.

Thank you!

LO

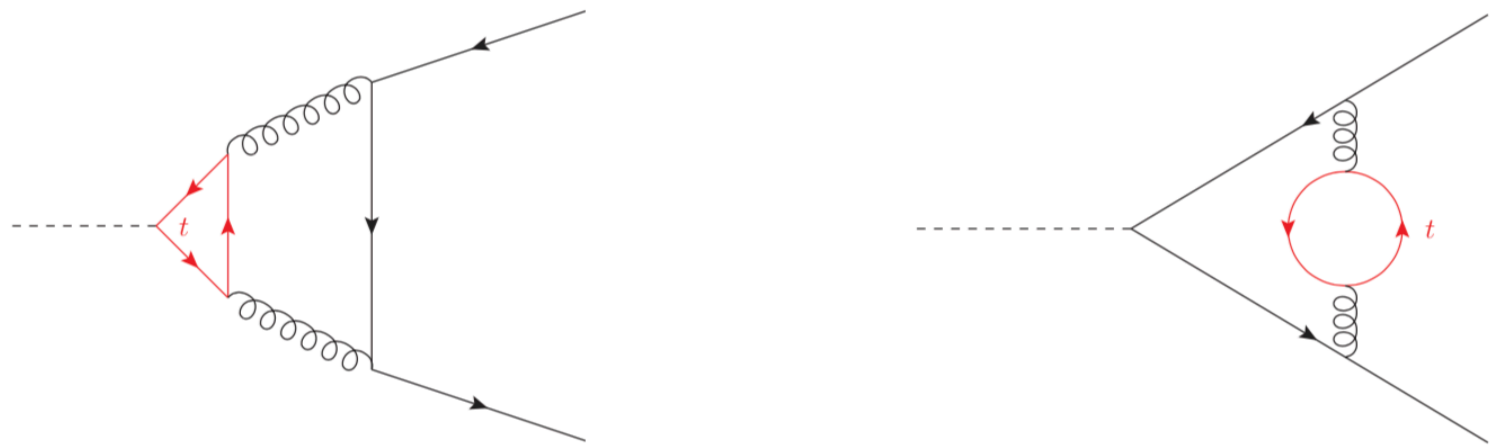

Figure 1. Representative top-quark loop contributions for the matching of the $Hq_L\bar{q}_R$ amplitude.

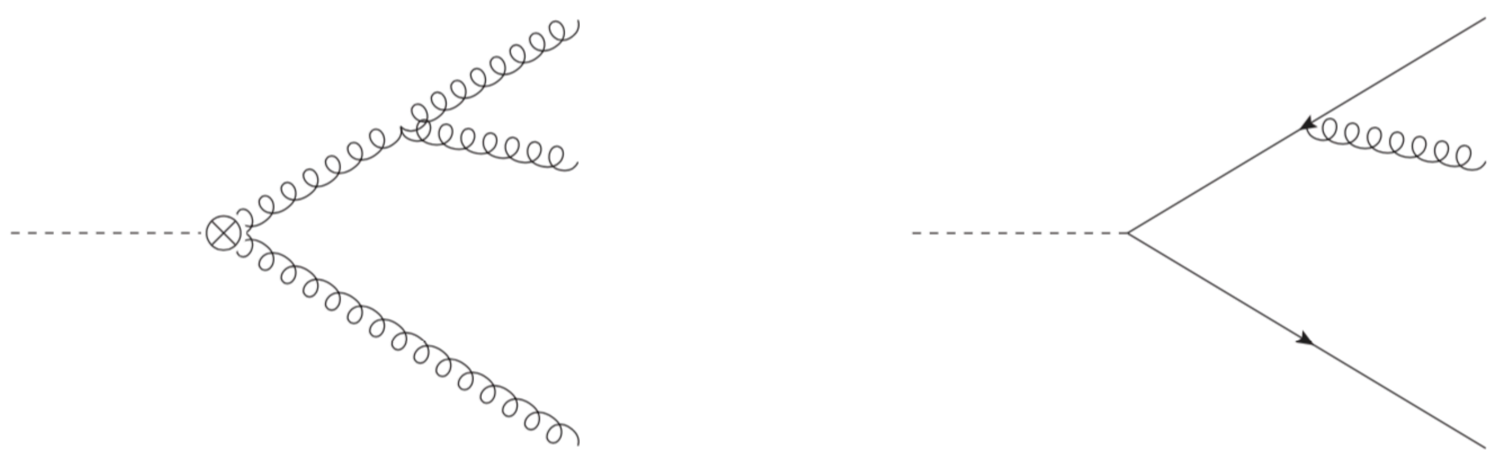

Figure 2. Representative Feynman diagrams for the Hgg channel (left) and the $Hq\bar{q}$ channel (right) for the thrust distribution at LO.

NLO

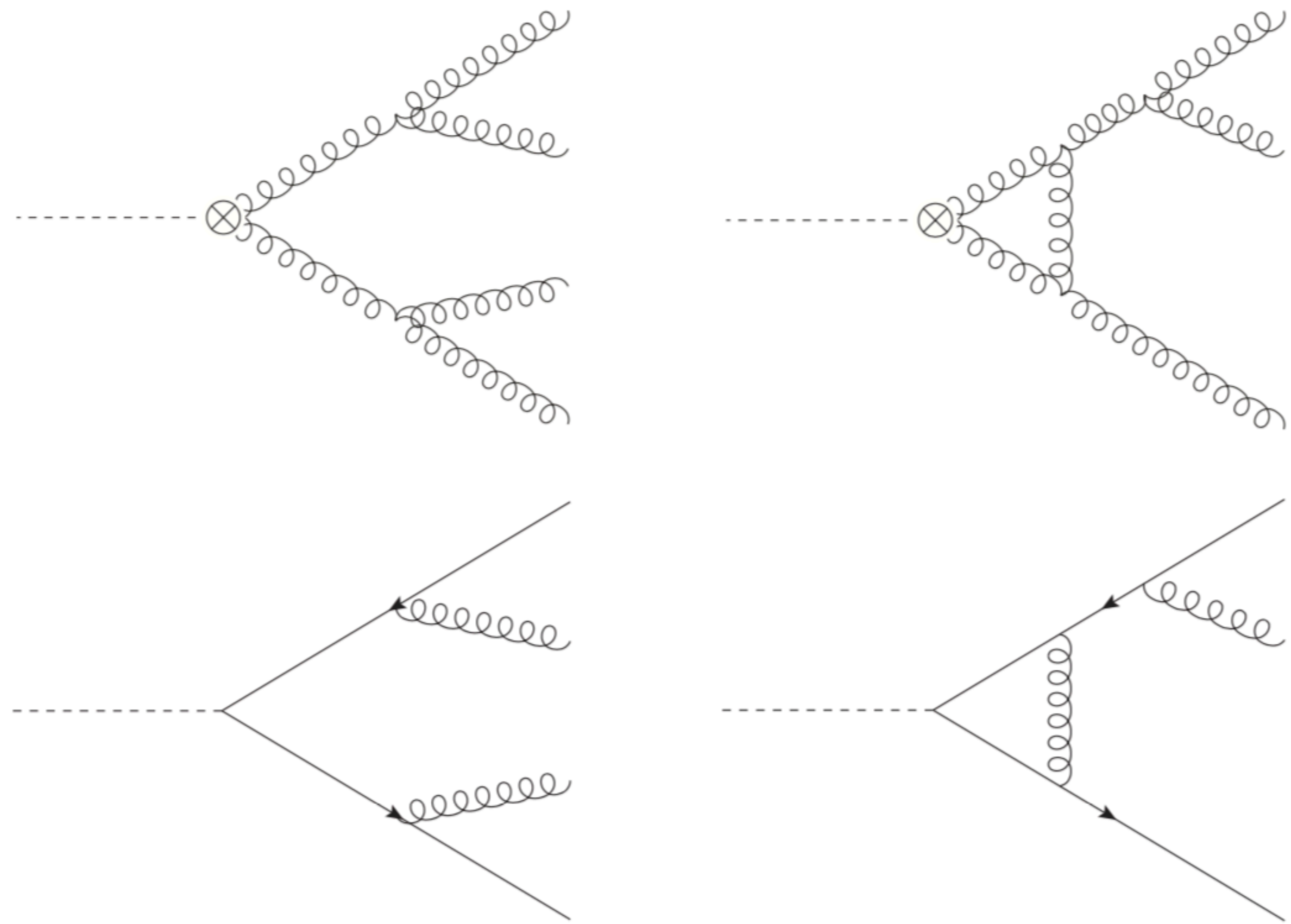

Figure 3. Representative Feynman diagrams for the Hgg channel (upper) and the $Hq\bar{q}$ channel (lower) at NLO.

Two-loop constant of gluon jet function

Full QCD

$$\frac{1}{\Gamma_B}\frac{d\Gamma}{d\tau_a} = A\delta\left(\tau_a\right) + \left[B\left(\tau_a\right)\right]_+ + r\left(\tau_a\right)$$

SCET

$$\frac{1}{\Gamma_B}\frac{d\Gamma_s}{d\tau_a} = A\delta\left(\tau_a\right) + \left[B\left(\tau_a\right)\right]_+$$

Total decay rate

$$\frac{\Gamma_t}{\Gamma_B} = \int_0^1 d\tau_a' \frac{1}{\Gamma_B}\frac{d\Gamma}{d\tau_a'} = A + r_c$$

Result: Two-loop Constant of gluon jet function

$c_{\tilde{J}}^2 \setminus a$	-1	-0.75	-0.5	-0.25	0
this work	44.19 ± 1.70	2.10 ± 2.75	-36.43 ± 1.65	-62.08 ± 2.49	-54.55 ± 2.60
Ref. [59]*	37.18	-4.59	-40.27	-56.95	-55.73
$c_{\tilde{J}}^2 \setminus a$	0.25	0.5			
this work	75.09 ± 10.99	814.48 ± 28.71			
Ref. [59]*	69.21	776.61			

Higgs decay rate h -> gg (Fixed order)

$$\frac{d\Gamma^i}{d\tau_a} = \Gamma_B^i(\mu)|C_t^i(m_t,\mu)|^2\,|C_S^i(m_H,\mu)|^2 \int d\tau_a^{J1}\,d\tau_a^{J2}d\tau_a^S\,\delta\Big(\tau_a-\tau_a^{J1}-\tau_a^{J2}-\tau_a^S\Big)$$
$$\times J^i(\tau_a^{J1},\mu)\,J^i(\tau_a^{J2},\mu)\,S^i(\tau_a^S,\mu)\,,$$

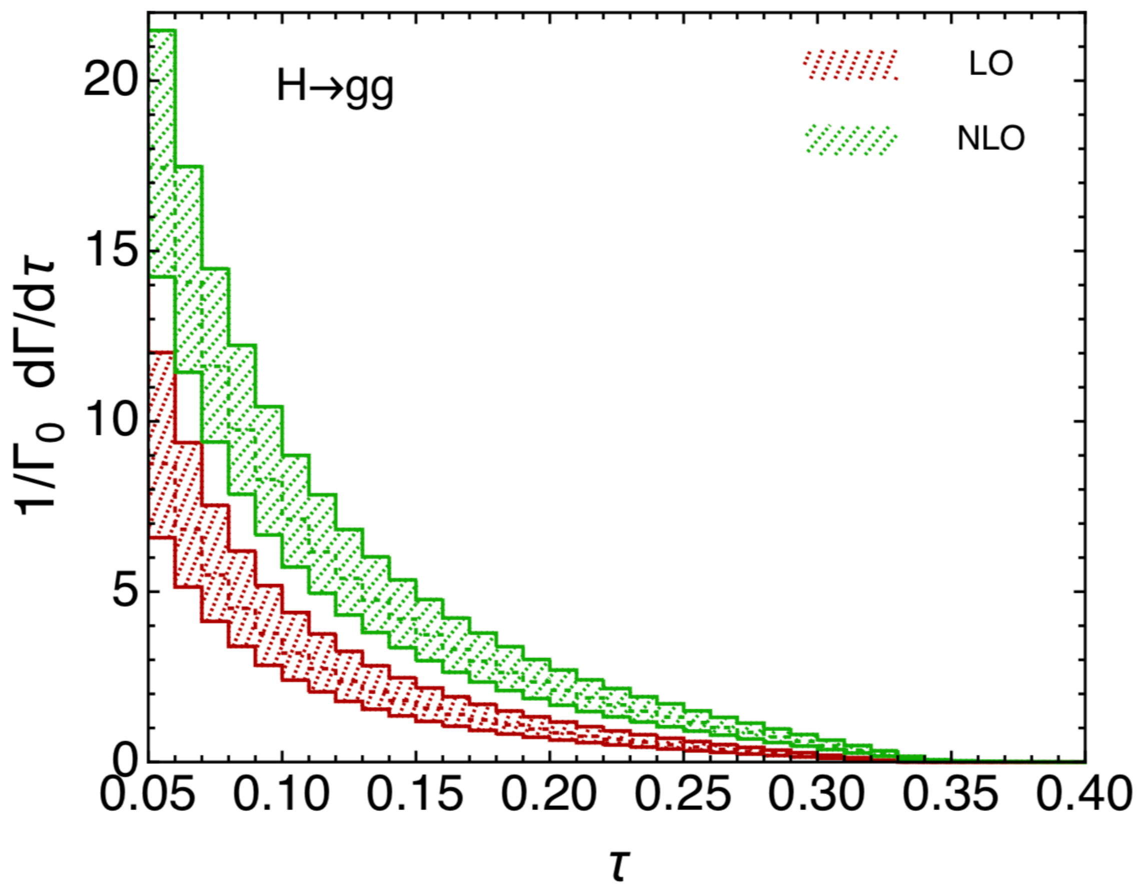

Fixed order pQCD result

Top-loop Contribution

Wilson coefficient $C_t(m_t, \mu)$ comes from integrating out the top quark, whose perturbative expansion can be written as

$$C_t(m_t, \mu) = 1 + \sum_{n=1}^{\infty} \left(\frac{\alpha_s(\mu)}{4\pi} \right)^n C_t^{(n)}(m_t, \mu) \,. \tag{2.3}$$

The coefficients $C_t^{(n)}(m_t, \mu)$ have been calculated up to N^{4}LO [46–52]. For our purpose, we need the results up to N^{3}LO, which are given by

$$\begin{aligned} C_t(m_t, \mu) = 1 &+ \frac{\alpha_s}{4\pi} 11 + \left(\frac{\alpha_s}{4\pi}\right)^2 \left[L_t \left(19 + \frac{16}{3} n_f \right) + \frac{2777}{18} - \frac{67}{6} n_f \right] \\ &+ \left(\frac{\alpha_s}{4\pi}\right)^3 \left[L_t^2 \left(209 + 46 n_f - \frac{32}{9} n_f^2 \right) + L_t \left(\frac{4834}{9} + \frac{2912}{27} n_f + \frac{77}{27} n_f^2 \right) \right. \\ &\left. - \frac{2761331}{648} + \frac{897943\zeta_3}{144} + \left(\frac{58723}{324} - \frac{110779\zeta_3}{216} \right) n_f - \frac{6865}{486} n_f^2 \right] , \end{aligned} \tag{2.4}$$

where $L_t = \ln(\mu^2/m_t^2)$, and we have set explicitly the number of colors $N_c = 3$ to shorten the expression.

Hard functions

We expand the hard Wilson coefficients C_S^i in eq. (4.1) as

$$C_S^i(m_H,\mu) = 1 + \sum_{n=1}^{\infty} \left(\frac{\alpha_s(\mu)}{4\pi}\right)^n C_S^{i(n)}(L_H)\,,$$

where

$$L_H = \ln \frac{-m_H^2 - i\epsilon}{\mu^2}\,.$$

The NLO and NNLO coefficients are given by [70, 71]

$$\begin{aligned}
C_S^{g(1)}(L_H) &= C_A\left(\frac{\pi^2}{6} - L_H^2\right)\,,\\
C_S^{g(2)}(L_H) &= C_A^2\left[\frac{L_H^4}{2} + \frac{11L_H^3}{9} + \left(\frac{\pi^2}{6} - \frac{67}{9}\right)L_H^2 + \left(-2\zeta_3 - \frac{11\pi^2}{9} + \frac{80}{27}\right)L_H\right.\\
&\quad \left. + \frac{\pi^4}{72} - \frac{143\zeta_3}{9} + \frac{67\pi^2}{36} + \frac{5105}{162}\right] + C_F n_f\left(2L_H + 8\zeta_3 - \frac{67}{6}\right)\\
&\quad + C_A n_f\left[-\frac{2L_H^3}{9} + \frac{10L_H^2}{9} + \left(\frac{52}{27} + \frac{2\pi^2}{9}\right)L_H - \frac{46\zeta_3}{9} - \frac{5\pi^2}{18} - \frac{916}{81}\right]
\end{aligned}$$

a < 0 and small-x result

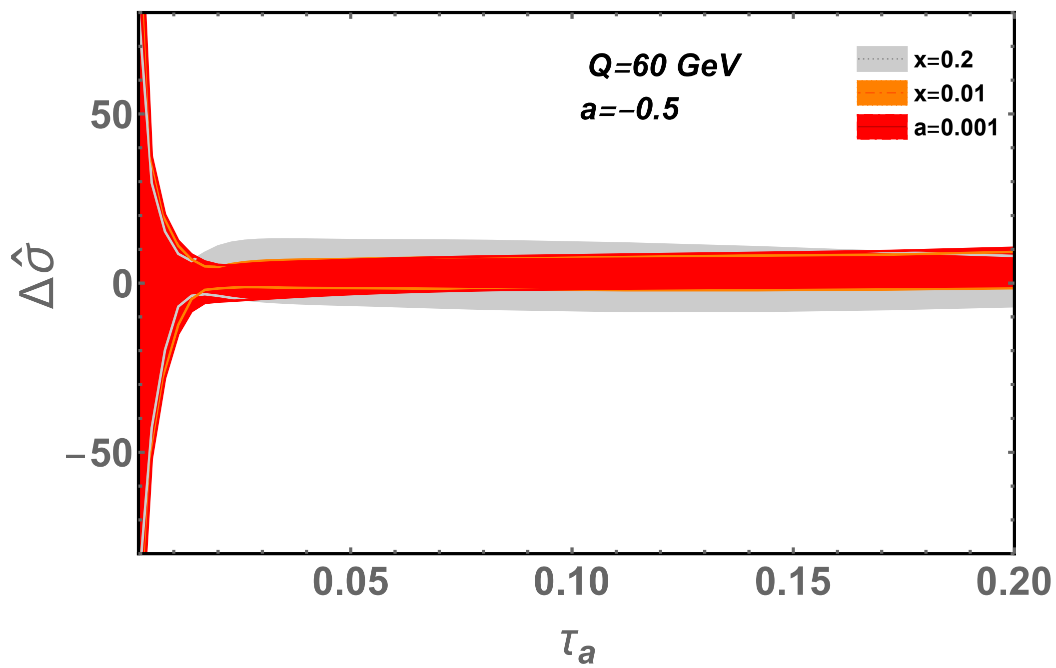

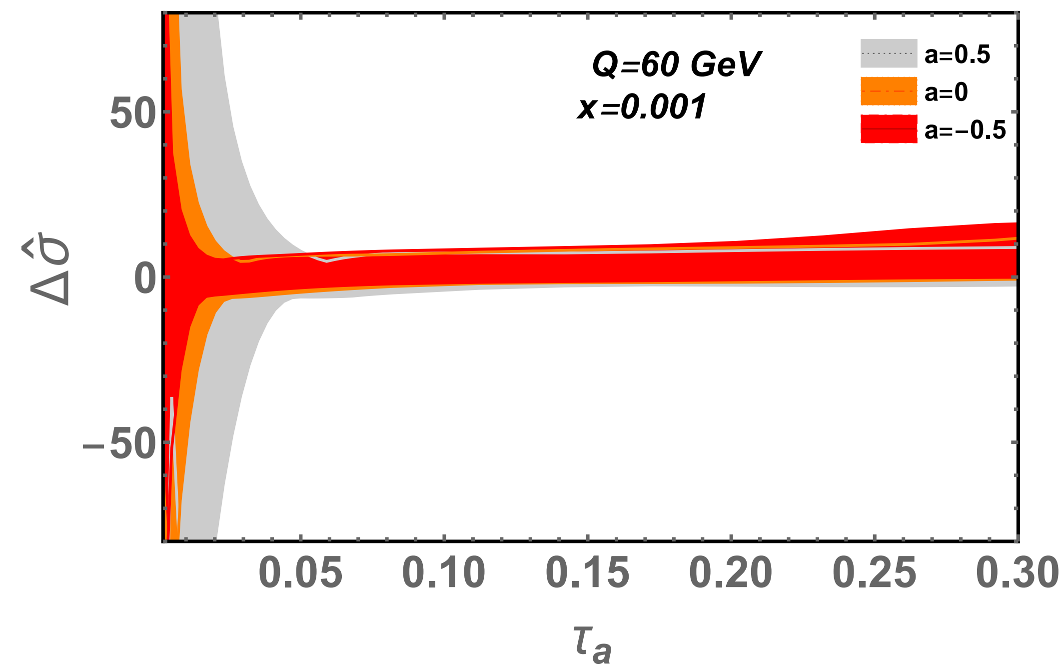

a < 0 and small-x result

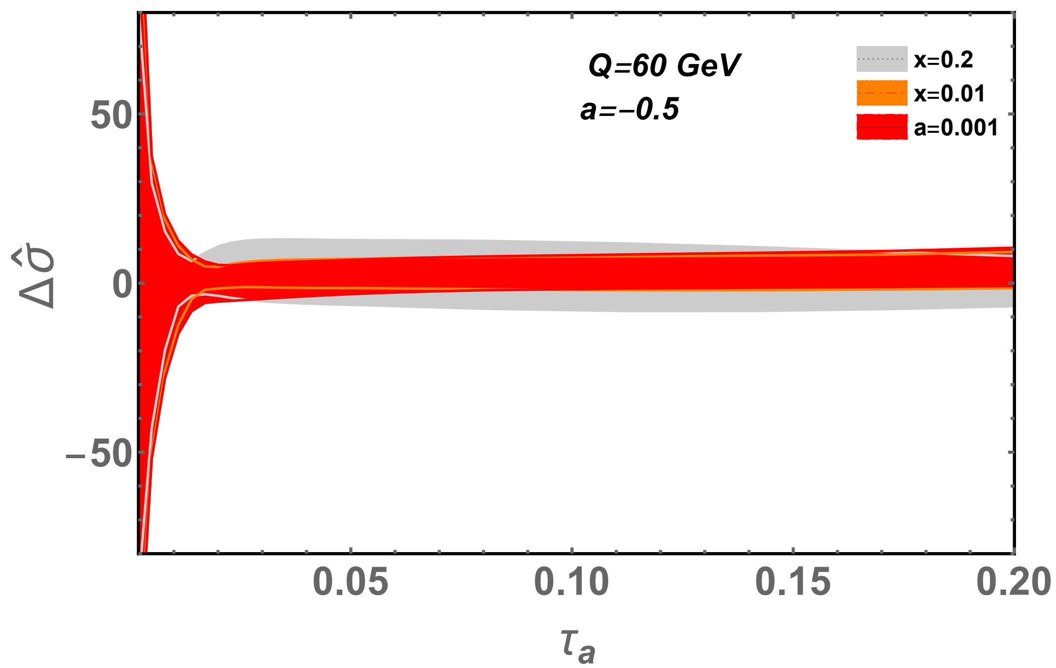

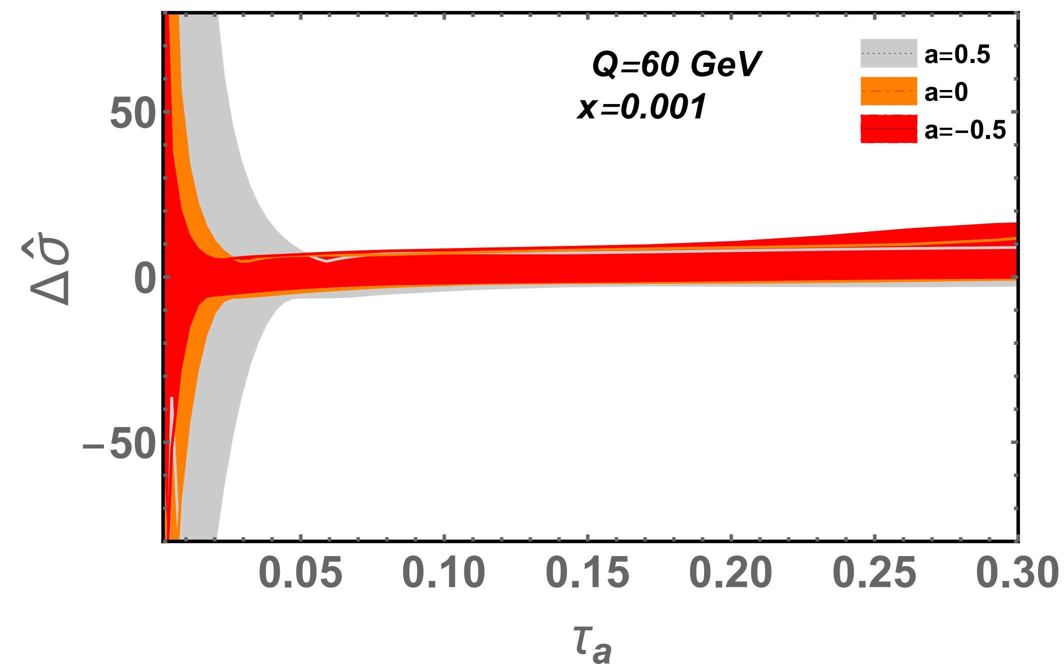

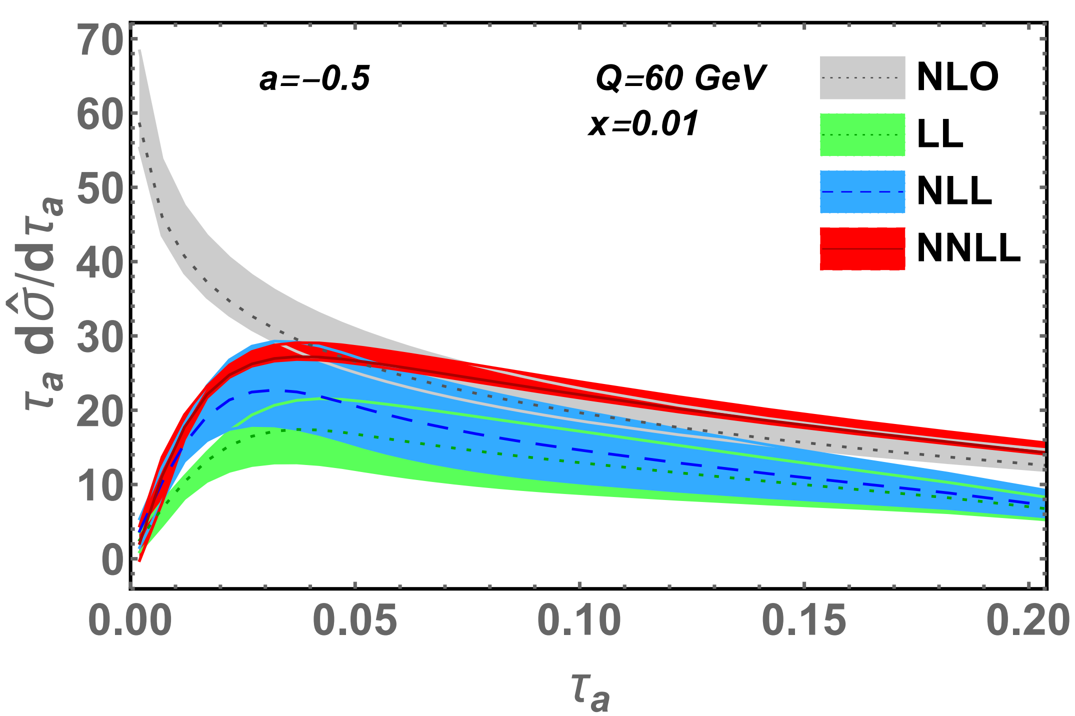

- Gluon contribution to the NLO correction is large at small-x region

a < 0 and small-x result

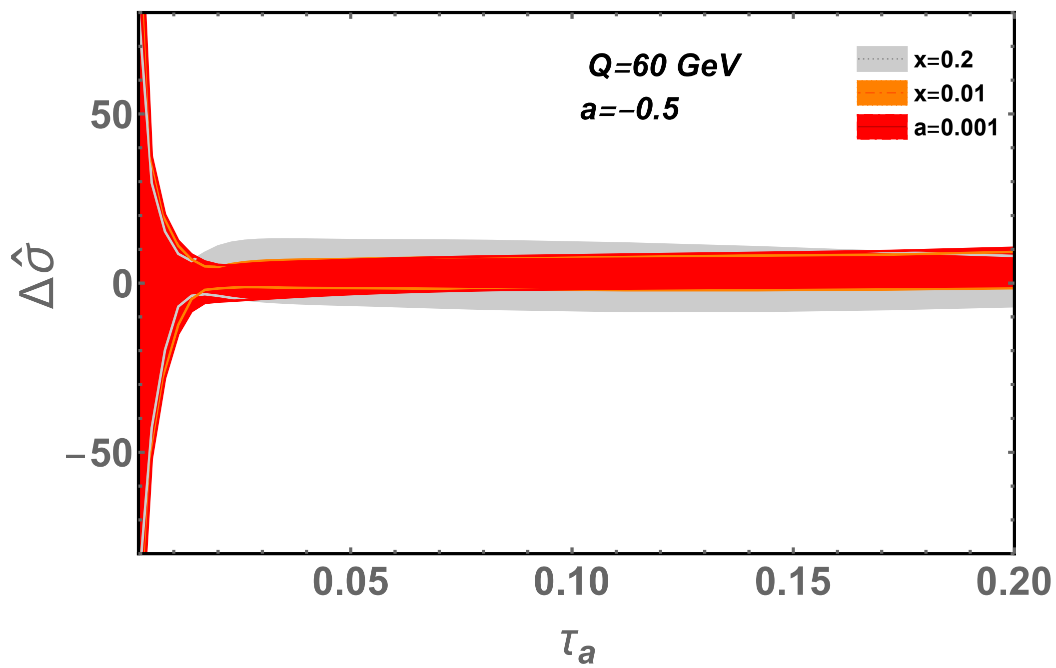

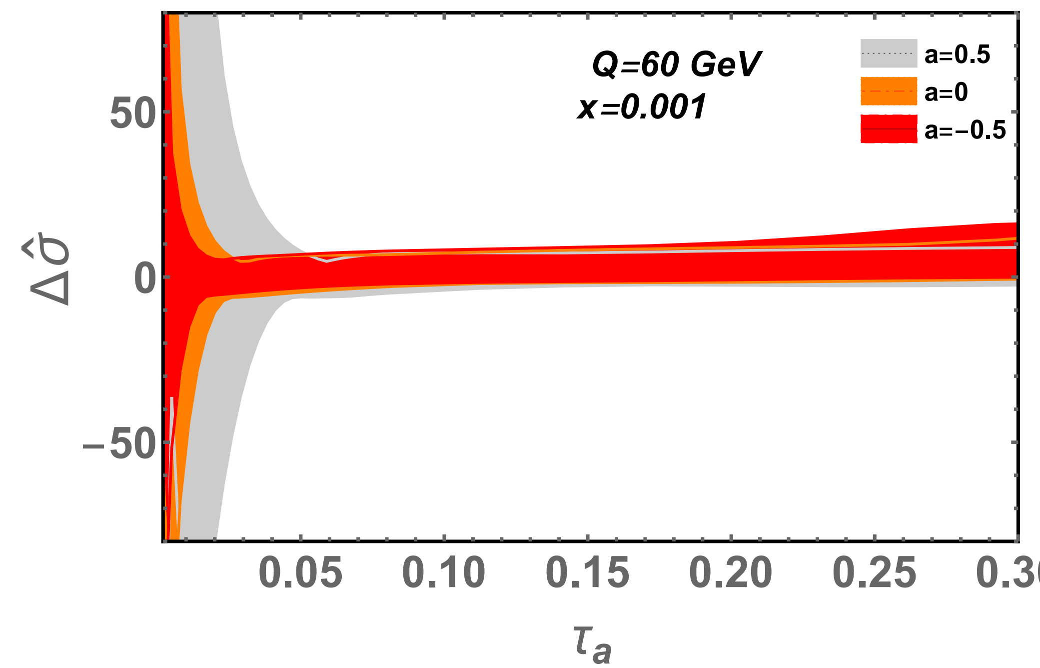

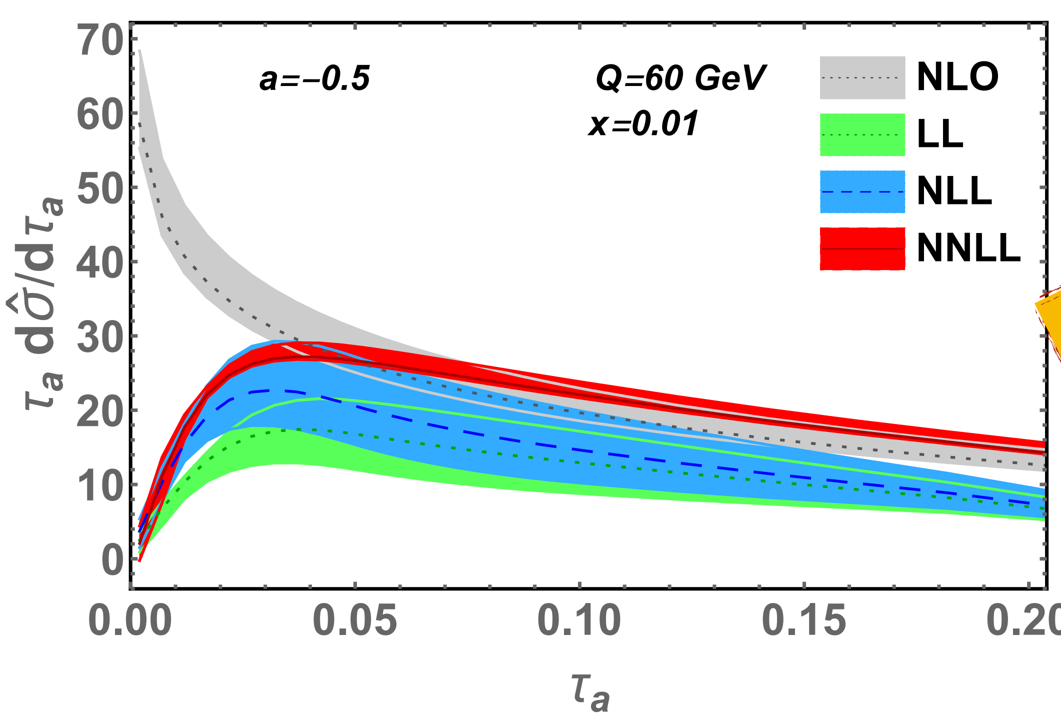

a < 0
&
small-x region

- Gluon contribution to the NLO correction is large at small-x region

Future direction

1. An extension of this work to access the entire α space, specially $\alpha \sim 1$ region, by incorporating the recoil effect.
2. Uncertainty in the cross-section is sensitive to Q, ’α’ and ‘x’ and we need to find out a reasonable profile function for DIS angularity.

Future direction

1. An extension of this work to access the entire **a** space, specially **a**~1 region, by incorporating the recoil effect.
2. Uncertainty in the cross-section is sensitive to Q, ’**a**’ and ‘x’ and we need to find out a reasonable profile function for DIS angularity.

1. Recoil effect in DIS angularity and access to the entire a space, specially **a**~1 region, by incorporating the recoil effect in DIS!!

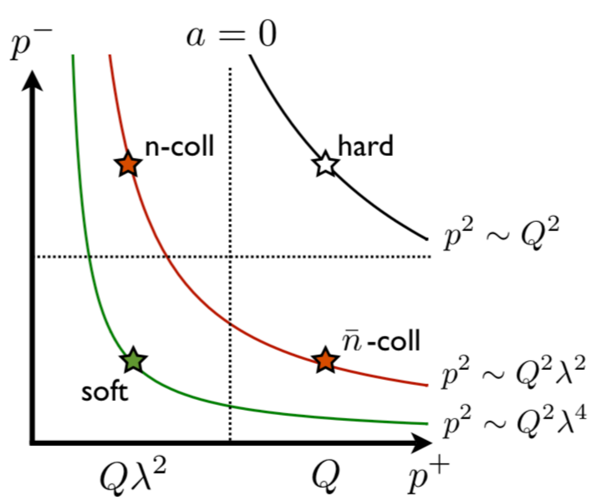

SCET-I

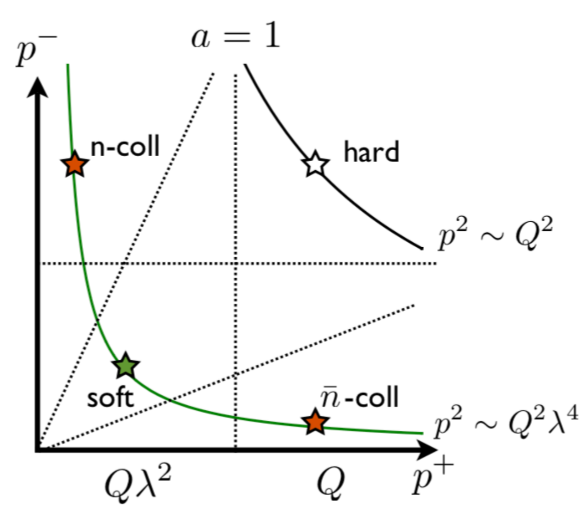

SCET-II

b=(1-a)

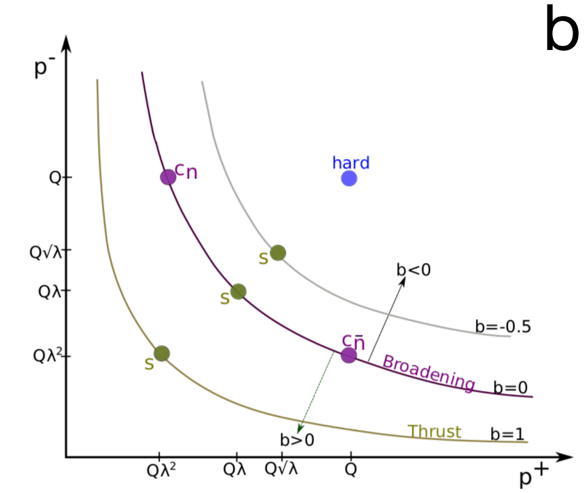

Recoil effect

—Andrew Hornig, Christopher Lee, and Grigory Ovanesyan,JHEP 05 (2009) 122

—A. Budhraja, Ambar Jain and Massimiliano Procura, JHEP08(2019)144

Anomalous dimension

The universal cusp anomalous dimension $\Gamma_{\rm cusp}(\alpha_s)$ and non-cusp anomalous dimension $\gamma_G(\alpha_s)$ are expressed in powers of α_s as

$$\Gamma_{\rm cusp}(\alpha_s) = \sum_{n=0} \Gamma_n \left(\frac{\alpha_s}{4\pi}\right)^{n+1} , \qquad \gamma_G(\alpha_s) = \sum_{n=0} \gamma_n^G \left(\frac{\alpha_s}{4\pi}\right)^{n+1} , \tag{4.15}$$

where Γ_n are given in appendix D and one-loop result for γ_n^G are given in [36]

$$\gamma_0^G = \{-12C_F\,, 0\,, 6C_F\} \qquad G = \{H, S, J\}\,, \tag{4.16}$$

which again satisfies the consistency in eq. (4.13) at the order α_s. The two-loop hard anomalous dimension is well known [61, 63] and available up to three-loops [64]

$$\gamma_1^H = -2C_F\Big[\Big(\frac{82}{9} - 52\zeta_3\Big)C_A + (3 - 4\pi^2 + 48\zeta_3)C_F + \Big(\frac{65}{9} + \pi^2\Big)\beta_0\Big]\,. \tag{4.17}$$

$$\gamma_G(\mu) = j_G\, \kappa_G \Gamma_{\rm cusp}(\alpha_s) L_G + \gamma_G(\alpha_s)\,, \tag{4.11}$$

where $\Gamma_{\rm cusp}(\alpha_s)$ and $\gamma_G(\alpha_s)$ are the cusp and non-cusp anomalous dimensions. The characteristic logarithm L_G is defined as

$$L_G = \begin{cases} \ln\left(\frac{Q}{\mu}\right) & G = H\,, \\ \ln\left[\frac{Q}{\mu}(\nu e^{\gamma_E})^{-1/j_G}\right] & G = \{\widetilde{S}, \widetilde{J}, \widetilde{\mathcal{B}}\}\,, \end{cases} \tag{4.12}$$

The consistency relation followed by scale independence of cross section $d\sigma(\mu)/d\mu = 0$ is given by $\gamma_H(\mu) + \gamma_{\widetilde{S}}(\mu) + 2\gamma_{\widetilde{J}}(\mu) = 0$, which is valid for any values of Q, μ, ν in eq. (4.11) and it turns into three consistency relations

$$\begin{aligned} j_H\, \kappa_H + j_S\, \kappa_S + 2 j_J\, \kappa_J &= 0\,, \\ \kappa_S + 2\kappa_J &= 0\,, \\ \gamma_H(\alpha_s) + \gamma_S(\alpha_s) + 2\gamma_J(\alpha_s) &= 0\,. \end{aligned} \tag{4.13}$$

The constants j_G and κ_G are given by

$$\begin{aligned} j_G &= \{1, 1, 2-a\}\ , \\ \kappa_G &= \left\{4, \frac{4}{1-a}, -\frac{2}{1-a}\right\}\ , \qquad\qquad G = \{H, S, J\} \end{aligned} \tag{4.14}$$

where $C_{qj} = C_F, T_F$ for $j = q, g$. One of the logarithmic terms L_B is associated with PDF with the splitting functions P_{qj}

$$\begin{aligned} P_{qq}(z) &= \left[\frac{\theta(1-z)}{1-z}\right]_+ (1+z^2) + \frac{3}{2}\delta(1-z) = \left[\theta(1-z)\frac{1+z^2}{1-z}\right]_+\ , \\ P_{qg}(z) &= \theta(1-z)[(1-z)^2 + z^2]\,. \end{aligned} \tag{5.5}$$

Profile function

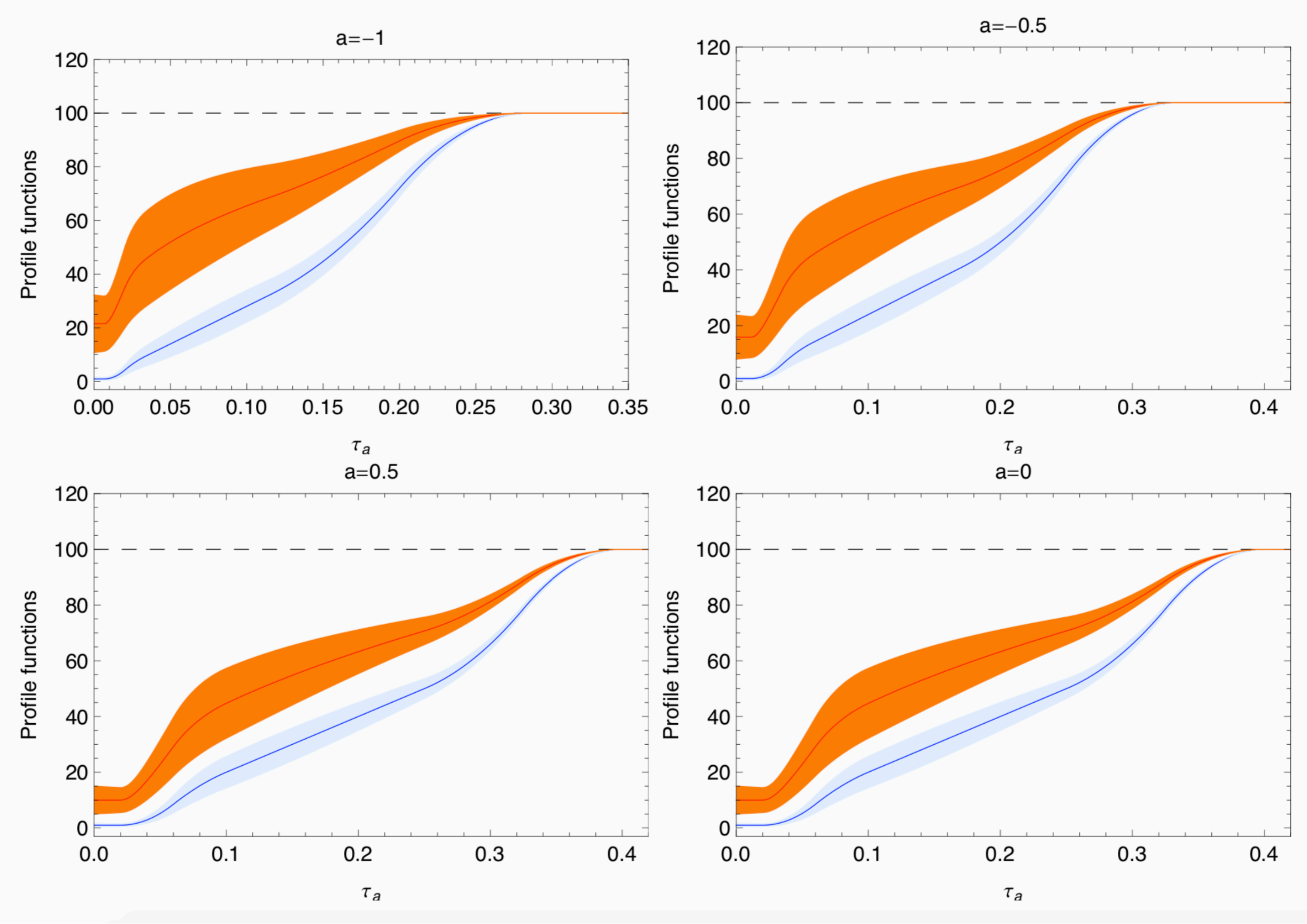

Profile function

- We adopt electron-positron angularity profile function from Bell, Hornig, Lee, Talbert, 18

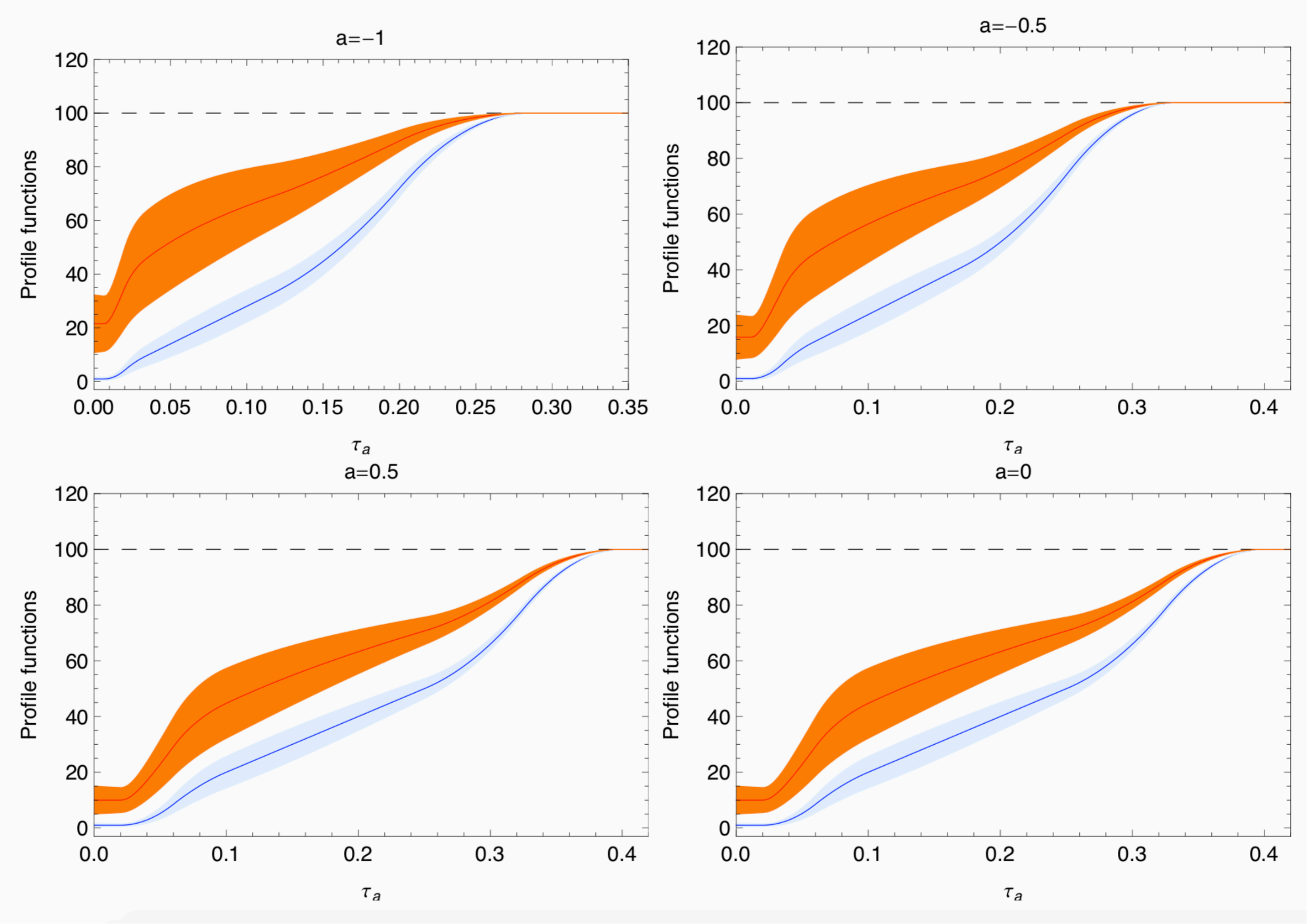

DIS factorization in SCET

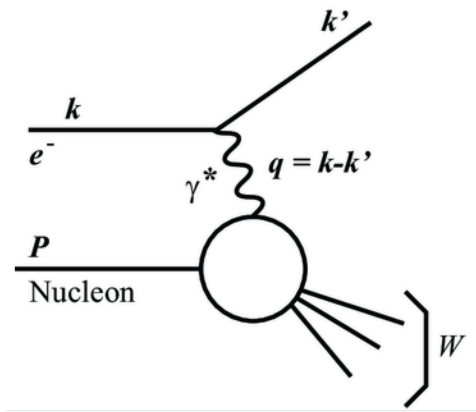

$$\frac{d\sigma}{dx\,dQ^2\,d\tau_a} = L_{\mu\nu}(x,Q^2)\; W^{\mu\nu}(x,Q^2,\tau_a)$$

The hadronic tensor defined by QCD current $J^\mu(x) = \bar\psi\gamma^\mu\psi(x)$

$$W^{\mu\nu}(x,Q^2,\tau_a) = \sum_X \langle P|J^{\mu\dagger}|X\rangle\langle X|J^\nu|P\rangle(2\pi)^{(4)}\delta^4(P+q-p_X)\delta(\tau_a-\tau_a(X))$$
$$= \int d^4x\, e^{iq\cdot x}\langle P|J^{\mu\dagger}(x)\delta(\tau_a-\hat\tau_a)J^\nu(0)|P\rangle\,.$$

Neglecting the power correction O(λ^2), we match the current $J^\mu(x) = \bar\psi\gamma^\mu\psi(x)$ onto the operators in SCET and perform the field redefinition to have factorized form of the hadronic tensor as

$$W_{\mu\nu}(x,Q^2,\tau_a) = \left(\frac{8\pi}{n_J\cdot n_B}\right)\int d\tau_a^J\,d\tau_a^B\,d\tau_a^S\,\delta\!\left(\tau_a-\tau_a^J-\tau_a^B-\tau_a^S\right)$$
$$\times H_{\mu\nu}(q^2,\mu)\mathcal{B}_i(\tau_a^B,x,\mu)J(\tau_a^J,\mu)S(\tau_a^S,\mu)$$

Measurement operator: $\hat\tau_a = \hat\tau_a^{cB} + \hat\tau_a^{cJ} + \hat\tau_a^S$

$$\boxed{\frac{d\sigma}{dx\,dQ^2\,d\tau_a} = \frac{d\sigma_0}{dx\,dQ^2}\int d\tau_a^J\,d\tau_a^B\,d\tau_a^S\,\delta\!\left(\tau_a-\tau_a^J-\tau_a^B-\tau_a^S\right) \times \sum_{i=q,\bar q} H_i(Q^2,\mu)\mathcal{B}_i(\tau_a^B,x,\mu)J(\tau_a^J,\mu)S(\tau_a^S,\mu)}$$

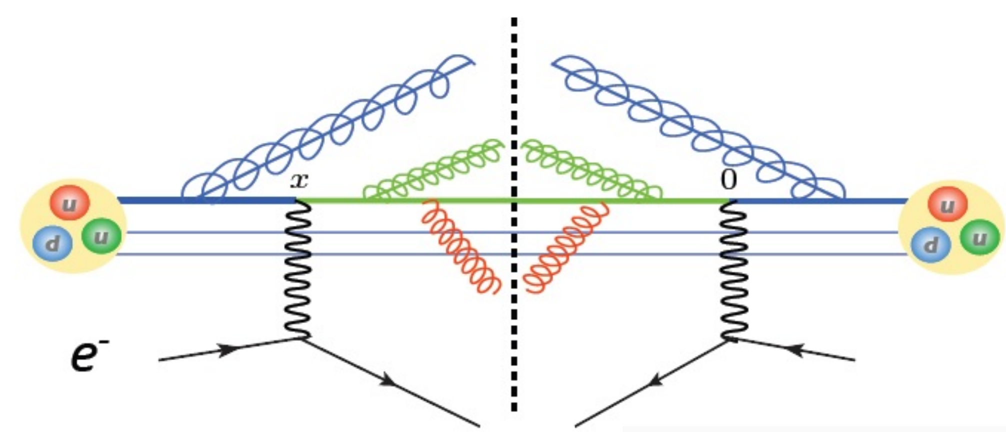

— D.Kang,Lee,Stewart'2013
Z.Kang,Mantry,Qiu'2012

SCET facto.: dσ = Hard × Beam ⊗ Jet ⊗ Soft